# Spatial Organization of Local Inputs to Spiny Projection Neurons in the Striatum

# Spatial Organization of Local Inputs to Spiny Projection Neurons in the Striatum

Jessica Lizette Saulnier

A Thesis in the Field of Biology

for the Degree of Master of Liberal Arts in Extension Studies

Harvard University

November 2015

## Abstract

GABAergic interneurons are important for balanced activity of the principal projection neurons of the striatum (spiny projection neurons, SPNs) and dysfunction of striatal GABAergic interneurons can lead to movement-related disorders. Despite this importance, very little is known about the connectivity of striatal interneurons and their functional spatial arrangement. In preliminary experiments, using optogenetics we identified a group of interneuron connections that had not previously been seen in paired recordings. Here we tested the hypothesis that this finding is due to long-range connections of genetically defined interneuron classes. Using a pseudotyped Rabies Viral (RV) monosynaptic retrograde tracing strategy in sparsely identified SPNs, followed by three-dimensional reconstruction, we tested the spatial attributes of connections from different striatal interneuron classes, and lateral connections between SPNs.

Our results demonstrate the feasibility of an RV-dependent approach for local distance mapping and for the first time identify distinct projection properties of different striatal neuron classes. Importantly, our experiments reveal short, local connections of Fast Spiking (FS), but long-ranging projections of Low-Threshold Spiking (LTS) interneurons, which together form the majority of striatal GABAergic interneurons. These findings can resolve the opposing results from paired and optogenetic recordings and also suggest distinct signaling modalities for these two types of interneurons.

Dedication

For Maria

Acknowledgments

I would like to express my sincere gratitude to my work wife, Michelle, for always encouraging me, believing in me and being my biggest supporter and champion. I can't thank you enough for never letting me give up and believing for both of us when I thought this was impossible. I hope when we're old and grey we still leave the husbands at home to set out for adventures with endless laughter. You make life more fun.

To my minion, Karina, thank you so much for all of your hard work. I'm thankful for the opportunity to have gotten to know you; we made a great team, you excel in areas where I do not and we were unstoppable! If only you could organize my entire life! How amusing it was to hear when people overheard us talking it was like listening to one person talk to them self. #smh Thanks for keeping me grounded especially during those times when science got hard ;-)

To my friends, Lisa, Lisa, Lauren, Rachel, Guido and Aurélien, thank you guys for all of your love, support and …everything – too many things to mention but especially for the care packages, study buddy's, study breaks, and countless dinners. All of it helped get me through. To my mom and husband, Victor, as well as, the rest of my family, thank you for all of your loving patience and encouragement.

I would also like to thank my thesis director, Dr. Bernardo Sabatini, for allowing me to do this work in his lab. I was blessed to have had the opportunity to complete the work for my thesis while employed at Harvard Medical School. My heartfelt gratitude to the members of the Sabatini Lab who offered their support and wisdom, I appreciate all your kindness.

Last but by no means least, a great deal of thanks to Dr. Christoph Straub without whose knowledge, guidance, patience and support I could never have achieved this. Thank you for taking me under your wing and making all this possible. I am forever grateful.

Table of Contents

List of Tables

List of Figures

List of Supplemental Materials

List of Supplemental Tables

List of Supplemental Figures

# Chapter I

## Introduction

In order to frame our hypothesis and further understand striatal GABAergic microcircuits, we evaluated the primary literature for background and compared published results with our own preliminary data. In this section of the text, we present the important findings from the literature relevant to our question, compare them to our results and formulate our specific aims. The overall goal of this study is to explore specific properties of striatal GABAergic microcircuits that could potentially explain differences between published results and our own work.

## Basal Ganglia Circuitry

Neuronal function is mediated by individual neurons that connect to form functional circuits, making these specialized cells the fundamental units of the brain. A major circuit for motor learning and execution is formed by the structures of the Basal Ganglia (BG), a subcortical group of interconnected nuclei. The biggest nucleus in the BG, the striatum, forms the entry for neuronal signals into the BG circuit and it is comprised of GABAergic principal projection neurons (spiny projection neurons, SPNs) and local interneurons, both cholinergic and GABAergic. GABAergic interneurons mediate local information processing between projection neurons and they are required for normal BG function. Despite their importance, however, there is little known about how different GABAergic interneurons target other cells and the logic of their connectivity remains unknown.

The Basal Ganglia (BG) belong to the phylogenetically oldest parts of the brain (Steiner and Tsneng, 2010). The striatum (caudate nucleus and putamen), globus pallidus (GPe), substantia nigra (SNr), nucleus accumbens and subthalamic nucleus (STN) comprise the major components of the BG and the flow of information through the BG is depicted in Figure 1 below.

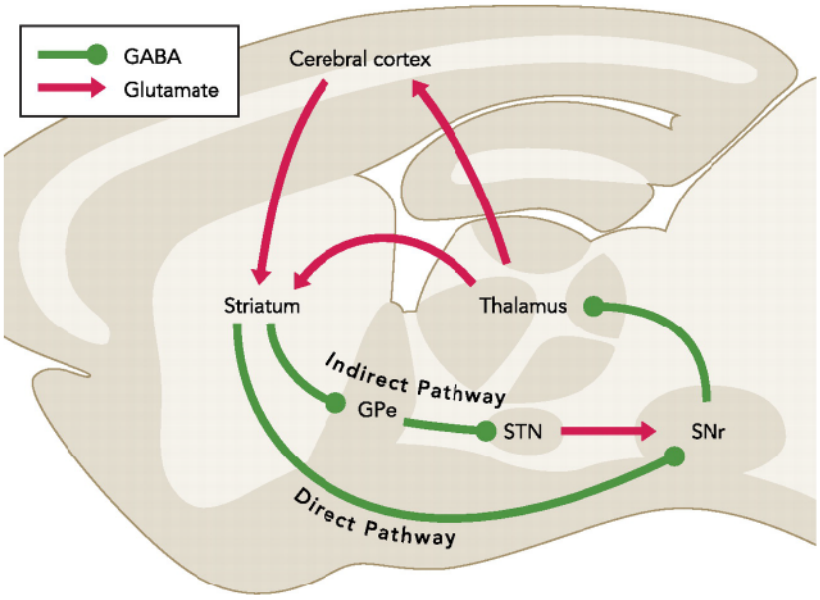


Figure 1. Diagram of the Basal Ganglia (BG)
Diagram shows the projections in the direct and indirect BG pathways. GPe, external globus pallidus; STN, subthalamic nucleus; SNr, substantia nigra pars reticulata (Modified from Kravitz and Kreitzer, 2012).

Studies in the last decade have significantly reshaped the canonical model of how the BG works. The current model describes BG function as a regulatory loop (Kozorovitskiy, 2012) through the different nuclei, in which input from the cortex ultimately conveys back onto cortex (Oldenburg and Sabatini, 2015). Within this loop, two parallel pathways of information flow exist and they are critical for motor function and procedural learning (Kreitzer, 2009). These signaling routes are initiated in the striatum by two different types of striatal projection neurons

('direct' and 'indirect', dSPNs and iSPNs, respectively) and form the direct and indirect pathways. They function in parallel to each other (Alexander and Crutcher, 1990) but have opposing net effects on the output structures (Kravitz *et al*., 2010). The activity in the BG is differentially controlled through these two pathways (Kozorovitskiy, 2012). The Substantia Nigra reticulata (SNr) is the output nucleus of both the direct and indirect pathway, but the two pathways have opposing net effects on SNr function. Ultimately, the direct pathway acts to drive thalamus by dis-inhibiting SNr, whereas the indirect pathways drives SNr function and thus inhibits thalamic drive onto cortex.

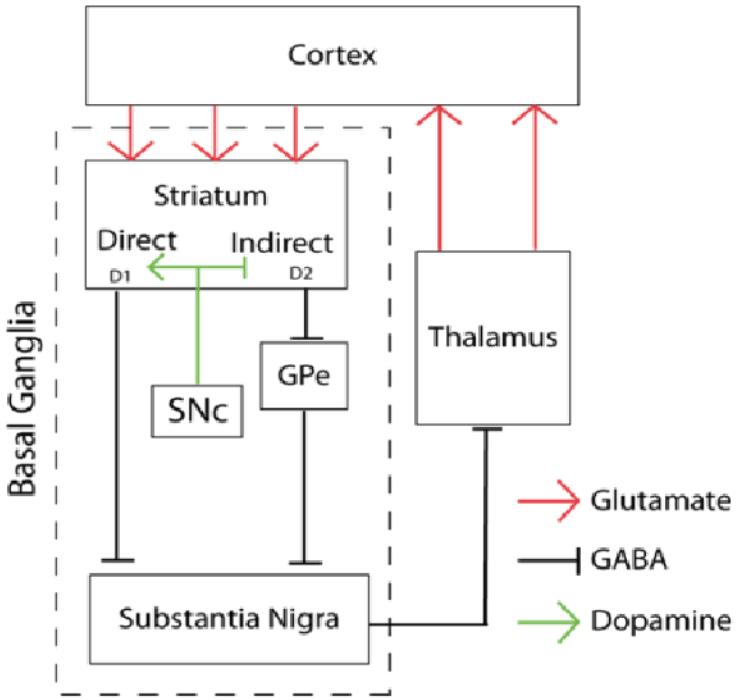


Figure 2. Basal Ganglia Connectivity Diagram
Glutamatergic pathways (red), inhibitory pathways (blue) and modulatory pathway as (green). GPe: globus palladus external; SNc, substantia nigra compacta.

For proper BG activity in these two parallel pathways must be balanced tightly (Neuroscience.uth.tmc.edu, 1). Dysfunction of the BG has been associated with a number of neurological disorders, including such illnesses as Parkinson's and Huntington's disease that display hallmark symptoms of severe motor impairment (Albin *et al.*, 1989; DeLong, 1990; Graybiel, 2000); and several of those motor-related BG disorders have been postulated to result from a disturbed balance between direct and indirect pathway (Neuroscience.uth.tmc.edu, 2). Understanding the workings of the BG in greater detail is thus of crucial importance, in order to better understand its role in neurodegenerative diseases.

## Striatum

The striatum forms the largest nucleus of the BG and provides its main input (Nelson and Kreitzer, 2014). Interestingly, it consists of only a few cell types and, unlike in other brain structures, the arrangement of these cells lacks any obvious spatial organization (Kawaguchi *et al*., 1995; Kreitzer, 2009) (Figure 3). Research over the past 25 years has led to significant progress in identifying different subclasses of neurons present in this region, yet several of these have not yet been fully described.

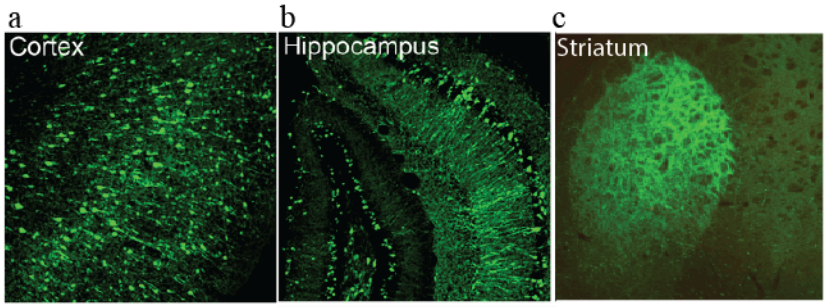


Figure 3. Cellular Organization
Viral expression of AAV-EGFP. Note the organization of dendrites in both the Cortex (a) and Hippocampus (b), but cannot be observed in Striatum (c) where cell bodies are not discernable ((a) and (b) Modified from McLean, 2014; (c) Modified from Korecka et al, 2011).

The principle cell type of the striatum is the GABAergic spiny projection neuron (SPN), which accounts for >90% of all striatal neurons (Kreitzer, 2009). Based on their projection pattern, SPNs are categorized as direct (projecting to substantia nigra reticulata, SNr) or indirect (projecting to globus pallidus external, GPe) and the two subtypes form two parallel loops. Interestingly, SPNs also form strong collateral synapses onto other SPNs, thereby mediating lateral inhibition (Tepper *et al.,* 2004). The remaining population of cells consists of local interneurons and historically, three major cell types have been classified by Kawaguchi and colleagues (Kawaguchi *et al.,* 1995): Cholinergic interneurons (CINs) which are large, aspiny cells that are spontaneously active and as such provide a constant tone of acetylcholine; and fast-spiking (FS) and low-threshold-spiking (LTS) interneurons which are both GABAergic interneurons with very different physiological properties.

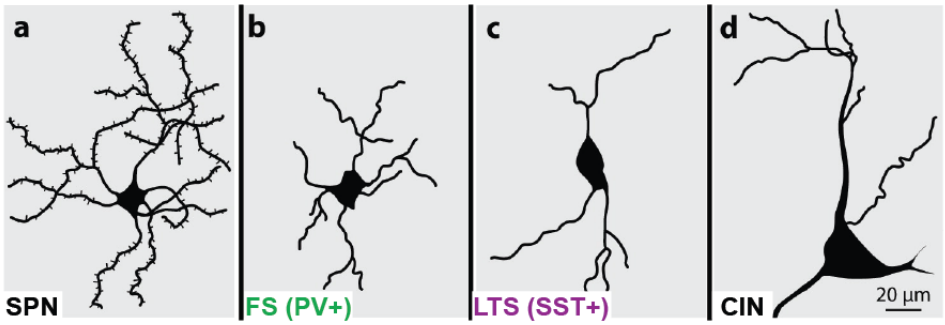


Figure 4. Four Major Cell Types of the Striatum
In addition to Spiny Projection Neurons (SPNs) (a), the striatum contains Cholinergic interneurons (CINs) (d), and two classes of GABAergic interneurons, Fast-Spiking (FS) (b) and Low-Threshold-Spiking (LTS) (d) interneurons (Modified from Kreitzer, 2009).

Besides these four major cell types, additional GABAergic interneuron subtypes might exist in the striatum (Tepper *et al.,* 2010), but their classification remains controversial. Striatal interneurons play crucial roles in the function of BG. Changes in their function are correlated with several neurological disorders and simply by inhibiting one class of GABAergic interneurons motor symptoms can be evoked in mice (Kaneko *et al.*, 2000; Pisani *et al.*, 2007; Gittis *et al*., 2011; Gittis and Kreitzer, 2012). However, despite their importance, the connectivity pattern and spatial organization of striatal GABAergic interneurons are poorly understood.

## Spiny Projection Neurons

SPNs, which release the neurotransmitter GABA, can be subdivided into two main classes based on gene expression and axonal projections (Kreitzer and Malenka, 2008). These classes of SPNs are called striatonigral (projecting directly to SNr) and striatopallidal (projecting to GPe) and make lateral connections onto each other (Reid, 1990). The former make up the direct (expressing the D1 dopamine receptor) and the latter, the indirect (expressing the D2

dopamine receptor) pathways. (Kreitzer and Malenka, 2008). The direct pathway (D1) is thought to help initiate or promote movements, whereas the indirect (D2) involves lack of movement initiation and freezing behaviors (Kreitzer and Malenka, 2008).

The creation of D1 receptor and D2 receptor transgenic mouse lines have enabled a more detailed examination of SPNs by specific labeling of cells from the respective pathways.

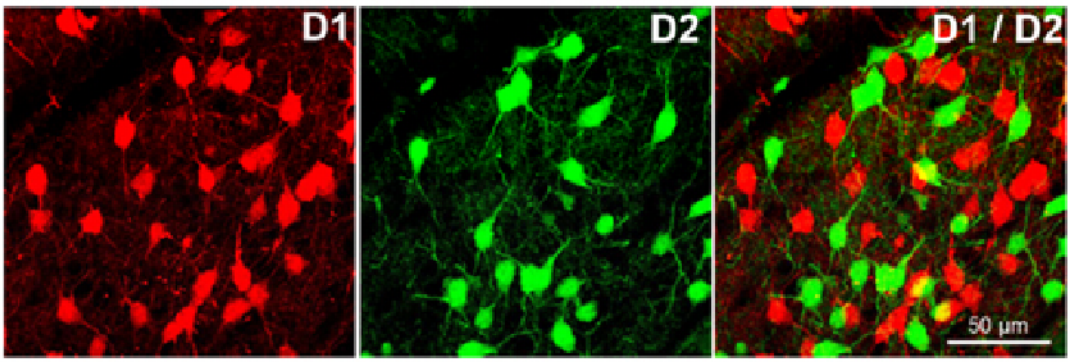


Figure 5. D1R and D2R Labeled Cells From BAC Transgenic Mouse Lines
D1 and D2 receptors are segregated in different cells in the striatum and in the nucleus accumbens. The first image (left) shows striatal cells of the direct striatonigral pathway expressing D1 receptors (specific reporter tdTomato under the control of D1R promotor). Second image (middle) show striatal cells of the indirect striatopallidal track expressing D2 receptors (specific reporter eGFP under the control of D2R promotor). The third picture (right) shows the lack of co-localization of D1 and D2 receptors in striatal cells (yellow parts of cells are cell overlap artifacts) (Modified from Del'Guidice, 2011).

dSPNs and iSPNs differ in their morphology in that the dendritic branches of D1 SPNs extend significantly further in length and have a higher degree of arborization than D2 SPNs (Steiner and Tseng, 2010). Another important morphological characteristic that has been examined are the dendritic spines of SPNs. These dense tiny projections are the sites of glutamatergic input to the striatum; they are involved in the plasticity of excitatory synapses and their shape may determine the action of excitatory inputs (Steiner and Tseng, 2010). While there

have been no significant differences discovered in the shape of dendritic spines found on D1 SPNs versus those on D2 SPNs (Steiner and Tseng, 2010), differences have been found in the way the spines react to levels of dopamine (Steiner and Tseng, 2010). In the D2 (striatopallidal) but not D1 (striatonigral) pathway, a decrease in the amount of local dopamine quickly results in a dramatic loss of dendritic spines and glutamatergic synapses (Steiner and Tseng, 2010).

Dopamine signaling plays a crucial role in the communication of striatal SPNs and is required for the movement process in order to facilitate the release of inhibition. In Parkinson's disease there is a breakdown in this communication between cells. The lack of dopamine contributes to the characteristic physical manifestations of this movement disorder, including tremors in the extremities and difficulty walking. Therefore, differences within the D1 and D2 pathways, as well as, further identification of the cellular architecture that make-up specific brain areas, is a very important pursuit in the field of neuroscience (Matamales *et al.*, 2009).

## Striatal Interneurons

The remaining 2-5% of the cell population in the striatum are aspiny interneurons and these include cholinergic and several classes of GABAergic cell types (Steiner and Tseng, 2010). These cells have axons that do not extend outside the perimeter of the striatum and while they are few in number, they play a large role in the information processing that occurs within the striatum (Steiner and Tseng, 2010). Local interneurons represent a class of cells that can be further sub-divided into groups and defined based on their morphological and physiological properties (Steiner and Tseng, 2010). First are the large aspiny interneurons, which propagate their signals through the neurotransmitter (NT) acetylcholine (ChAT) and are referred to as

Cholinergic Interneurons (CINs). Second are the medium aspiny cells that signal through the NT Gamma-Aminobutyric acid (GABA) (Steiner and Tseng, 2010).

Functionally, these GABAergic interneurons fall into two main classes, fast spiking (FS) and low-threshold spiking (LTS) interneurons (Kreizter, 2009). FS cells been further identified via immunohistochemistry as being positive for the small calcium binding protein, parvalbumin (PV+), while the LTS cells have been identified as being positive for somatostatin (SOM+), nitric-oxide synthase, neuropeptide-Y and possibly calretinin (Kawaguchi *et al*., 1995; Tepper and Bolam, 2004). Both types of interneurons, FS (PV+) and LTS (SOM+), are important for normal striatum function and further characterization of these sub-types is required.

## GABAergic interneurons

Patch-clamp electrophysiology is the most widely used method to examine cellular function and regulation of neurons (Liem *et al.*, 1995). This technique provides a method for recording ionic current through an intact cell for long periods of time by attaching a small glass pipette to an area of membrane (the "patch") (Liem *et al.*, 1995) and the selectivity of this method enables researchers to identify cell types based on their electrical activity. However, initial targeting relies on visual identification of individual cells and GABAergic interneurons make only 2-3% of all neurons within the striatum (Kreitzer, 2009). Without any morphologically specific characteristics it has been very difficult to target those cells in electrophysiological recordings and this technical problem accounts for the lack of knowledge in striatal interneuron function.

The first study to circumvent this problem utilized transgenic mice, which express GFP (green fluorescent protein) under the control of the developmental factor Lhx6 (*Lhx6-GFP*

mice). This factor is required for the development of GABAergic interneurons and hence labels all GABAergic interneurons (Gong *et al.*, 2003). In an attempt to characterize the downstream targets of GABAergic interneurons in the striatum, Gittis *et al.* combined this mouse line with electrophysiological patch-clamp recordings between GABAergic interneurons and spiny projection neurons (SPNs). They employed these tools to then classify targeted GABAergic interneurons electrically as FS or LTS (Gittis *et al.,* 2010).

With each targeted interneuron, a second recording was performed in parallel from an SPN ("paired recording") and this experimental set-up allowed testing connectivity between pairs of individual GABAergic interneurons and principal projection neurons. This approach revealed strong, reliable connection between FS interneurons and SPNs, but no connection was found between LTS interneurons and SPNs (or between LTS and any other striatal cell type). A second, independent study confirmed these results (Cepada *et al.*, 2013) and together these results raise questions about the identity of postsynaptic targets of LTS interneurons and about the function of this class of GABAergic interneuron in striatal circuitry.

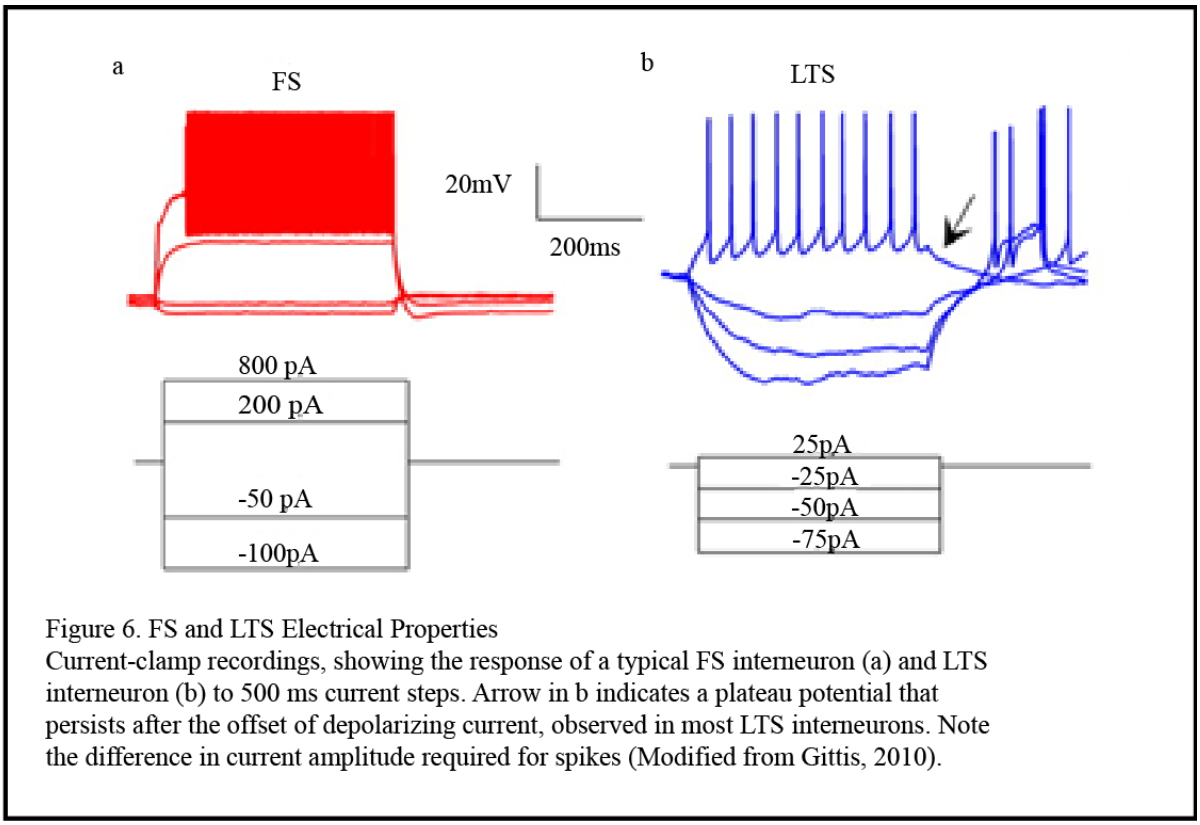


Figure 6. FS and LTS Electrical Properties
Current-clamp recordings, showing the response of a typical FS interneuron (a) and LTS interneuron (b) to 500 ms current steps. Arrow in b indicates a plateau potential that persists after the offset of depolarizing current, observed in most LTS interneurons. Note the difference in current amplitude required for spikes (Modified from Gittis, 2010).

## Introduction to Optogenetics

In 2005, the activity of a naturally occurring microbial protein was harnessed and introduced into neurons where it conferred millisecond precision control of neuronal spiking. Since then light-activated ion-channels of microbiological origin have been engineered to express in mammalian neurons in a genetically defined manner and if these channels conduct cations, the resulting current will depolarize the cell, leading to the generation of action potentials (Yizar *et al.*, 2011). This approach was termed "optogenetics" (Deisseroth *et al.*, 2006) and enables fast, precise control of neuronal populations by light. With this technique, neurons are genetically altered to express these light sensitive proteins, termed opsins. The activity of these cells can then transiently be modified when exposed to light of the correct wavelength. Depending on which particular type of opsin is expressed, the cells can be activated,

inhibited, or their signaling pathways can be modulated. Using this technique in transgenic animals allows for particular refinement in targeting the activity of neurons in specific brain regions.

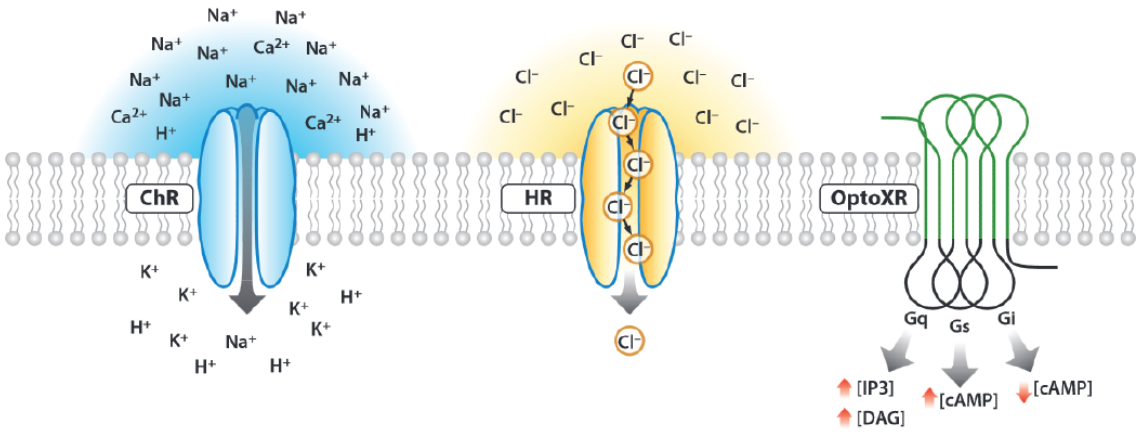


Figure 7. Optogenetic Tool Families
Channelrhodopsins conduct cations and depolarize neurons upon illumination (left). Halorhodopsins conduct chloride ions into the cytoplasm upon yellow light illumination (center) leading to hyperpolarization. OptoXRs are rhodopsin-GPCR (G protein-coupled receptor) chimera that respond to green (500nm) light with activation of the biological functions dictated by the intercelluar loops used in the hybrid (right) (Modified from Fenno, *et al.*, 2011).

## Re-Assessing Striatal GABAergic Interneurons with Optogenetics

Previous studies have relied on electrical activation of individual striatal GABAergic interneurons. Recent advances in the development of both mouse genetic and light-controlled proteins provide now the opportunity to simultaneously control the activity of several GABAergic interneurons of the same type and re-assess their impact on circuit function.

In parallel to the development of optogenetics, mouse genetics has matured to a degree that there are now mouse lines available that express the recombinase Cre in nearly every interneuron cell type. These lines utilize the expression of specific marker proteins in different

cell types and are genetically engineered to co-express Cre together with the respective marker proteins. FS interneurons in the striatum are known to specifically express parvalbumin (PV) and LTS interneurons express somatostatin (SOM) (Kreitzer, 2009), Therefore, *PV-Cre* or *SOM-Cre* mice (Madisen *et al.*, 2010 and Taniguchi *et al.*, 2011) express Cre exclusively in FS or LTS interneurons, respectively.

The expression of the light-gated cation channel, channelrhodopsin (ChR2), can be rendered Cre-dependent and under these conditions only cells expressing Cre will express ChR2 and will thus be light-controlled. Combining *PV-Cre* or *SOM-Cre* mice with Cre-dependent ChR2 expression therefore allows controlling the activity of striatal FS or LTS interneurons by light, respectively, without affecting other cells in the circuit.

Using this approach, our group found reliable connections between both FS and LTS interneurons and SPNs (Figure 2) and this finding is in direct contrast to the earlier paired-recording studies from Gittis *et al*.

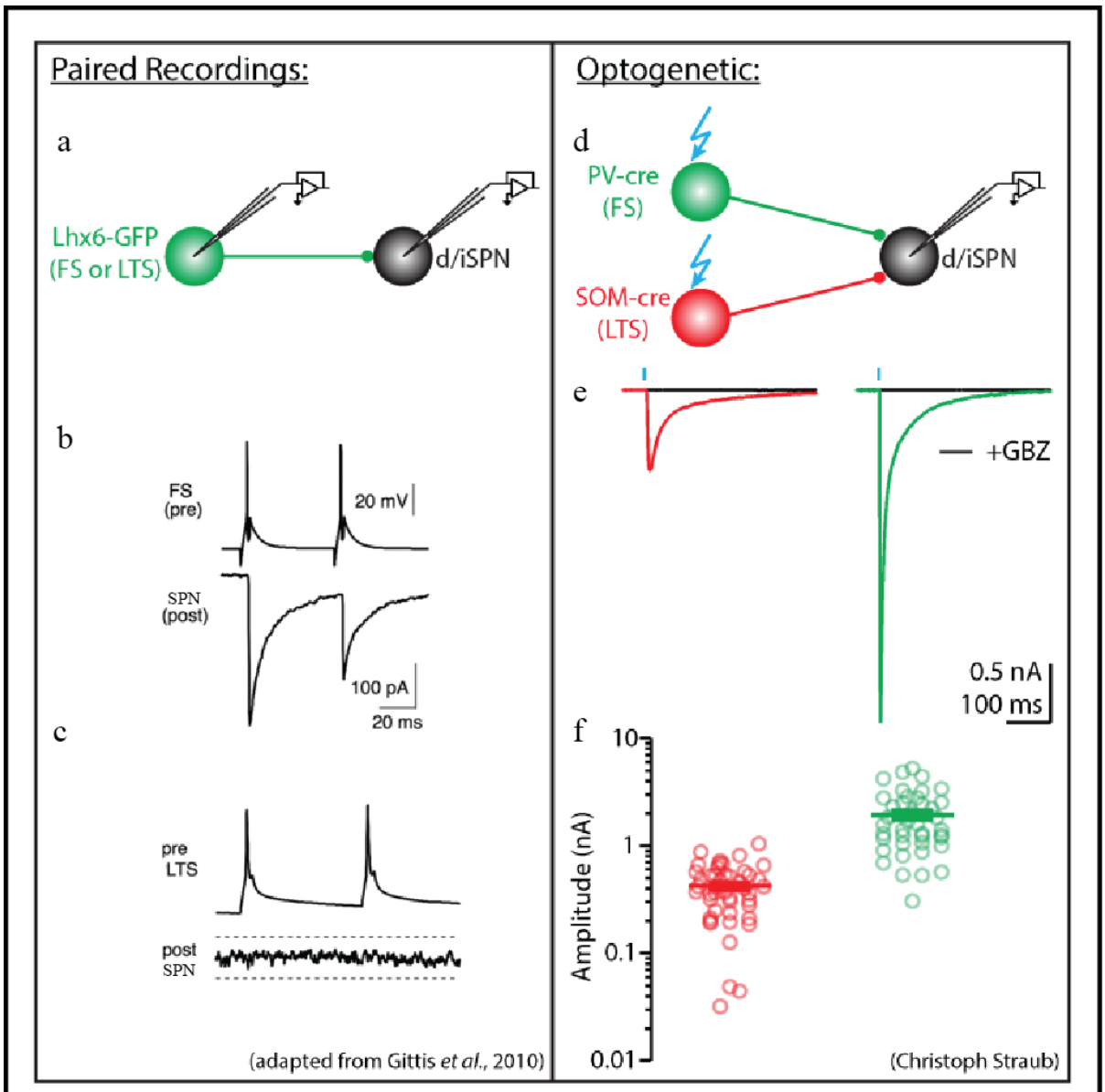


Figure 8. Conflicting Results From Paired Patch-Clamp and Optogenetic Recordings
(a,d) Experimental set-up. For paired recordings (a), an Lhx6-GFP expressing neuron and a neighboring SPN were targeted for simultaneous recording. Following electrical identification of the interneuron type (FS or LTS interneuron), connectivity was tested by eliciting an action potential in the the presynaptic interneuron and the postsynaptic response in the SPN was recorded. For optogenetic recordings, channelrhodopsin was expressed in *SOM-Cre* (labeling LTS interneurons) or *PV-Cre* (labeling FS interneurons) mice, and the postsynaptic response following light-activation of the respective interneruon was recorded in SPNs. (b,c,) In paired recordings, FS interneuron activation elicited a reliable postsynaptic response (b), but no response was detected following LTS interneuron activation (c). In contrast, optogenetic activation of LTS and FS interneurons evoked reliable responses from both interneuron types (e,f). (e) Black line indicates application of gabazine, a specific antagonist of GABA-A receptors.

This discrepancy raises the question why optogenetic activation of GABAergic interneurons, but not in paired recordings, yields reliable connectivity from all GABAergic interneurons, including LTS interneurons.

## Morphology of Striatal GABAergic Interneurons and Connection Distance

Established morphological characteristics of FS interneurons in different brain regions suggest that their innervation of postsynaptic targets creates particularly powerful inhibition because of the large number of target cells in close proximity to the site of action potential (Hu *et al.*, 2014). In agreement with this, striatal FS interneurons have been described anecdotally to form very short but highly branched axons, thereby forming a local "basket" around their target cells (Kawaguchi, 1993). In contrast to this, striatal LTS interneurons make sparsely branched axon that can extend over long distances. Kawaguchi described this cell type as having "the longest axon of all striatal interneurons… extending up to more than 1mm in radial distance…" (Kawaguchi, 1993).

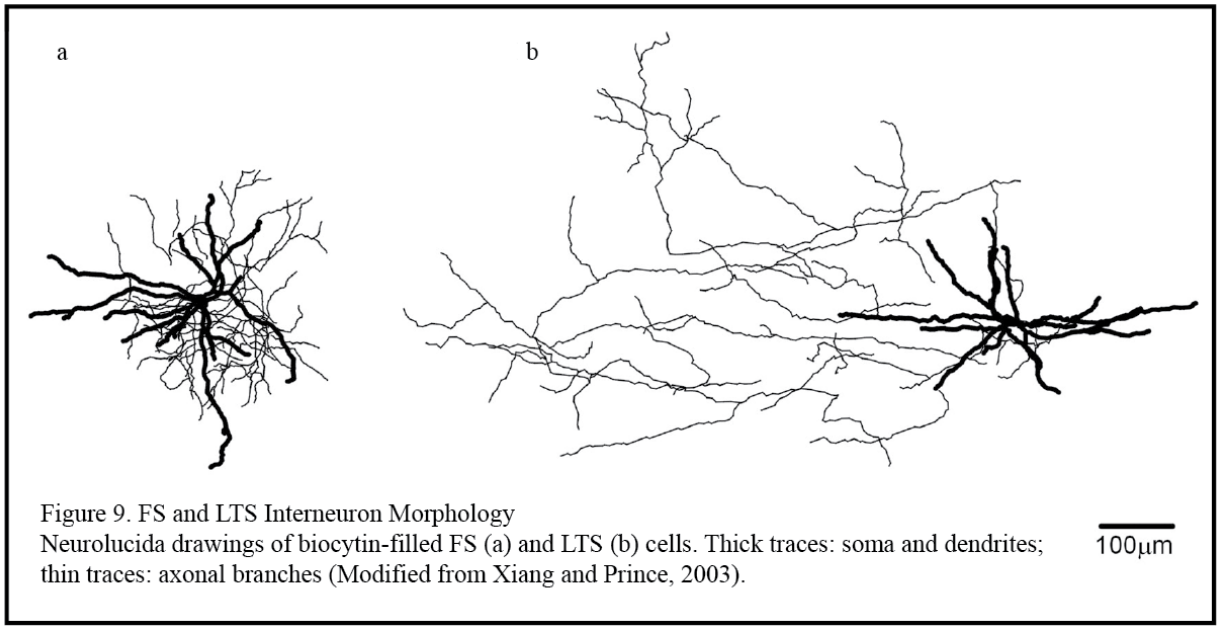


Figure 9. FS and LTS Interneuron Morphology
Neurolucida drawings of biocytin-filled FS (a) and LTS (b) cells. Thick traces: soma and dendrites; thin traces: axonal branches (Modified from Xiang and Prince, 2003).

As stated previously, paired recordings are performed between two cells that have a limited distance between them, while optogenetic activation occurs through the objective of a microscope and consequently activates all the cells within a particular field of view. Gittis *et al*. reported collecting data from cell pairs within a 250 μm maximal distance (average distance 153 ± 80 μm) (Gittis *et al.*, 2010), while the microscope used in our group activates a field measuring ~1.5 mm in diameter (C. Straub, personal communication).

Based on the anatomical difference in axonal anatomy of striatal GABAergic interneurons and given the different outcome of local paired recordings and wide-field optogenetic activation, I therefore propose that FS cells preferentially make nearby connections to SPNs, while LTS interneurons make distant connections onto SPNs and that our results reflect a new more accurate representation of striatal spatial organization.

The aim of this project is to test this hypothesis. To do so, we will use a monosynaptic, retrograde rabies virus system in a transgenic mouse model to map the local input of genetically defined neurons in the striatum and define the spatial logic of GABAergic input to SPNs.

## Viral Circuitry Mapping

Using viruses to label cells within the central nervous system (CNS) is proving to be an effective approach for mapping local and long-range connections. Previously, viruses from the herpes simplex family have been used as a neuronal tracing tool, to infect cells with a virus carrying a fluorophore, allowing transfer of genetic material to recipients and visualization of infected cells (Zampieri, 2014). This requires a small volume of virus to be injected into a desired brain region, thereby labeling all infected cells. This does not, however, limit the

subsequent spread of infection as cells are able to trans-synaptically pass on the virus making this approach an inefficient mapping tool. Recently it has been shown that rabies virus (RV) is a more suitable and reliable circuitry tracer (Zampieri, 2014).

Using genetic manipulations, RV can be modified to allow for retrograde transfer from the initial cell of infection across one synapse and into a target cell. This approach allows for more specific tracing by only infecting molecularly identified recipient cells (Zampieri, 2014). One group made a pseudotyped RV where the particle's viral coat was changed to an envelope that only allows the virus to recognize and infect cells containing the avian TVA receptor (Zampieri, 2014). RV can then be injected directly into transgenic mice bearing TVA receptors in certain populations of cells (Zampieri, 2014), or in combination with a "helper" virus that is injected first to convey the TVA receptor to targeted brain areas.

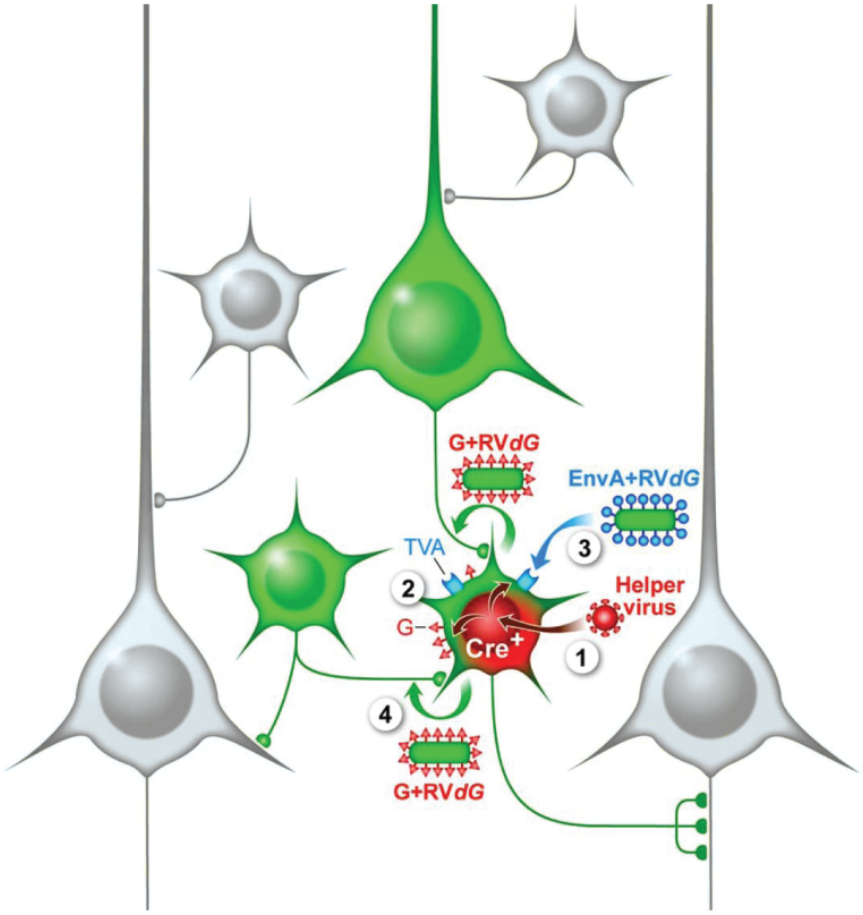


Figure 10. Monosynaptic Rabies Tracing of Inputs to Cre-Expressing Starter Cells
Monosynaptic tracing with G-deleted rabies (RVΔG) involves expression of the EnvA receptor, TVA, and rabies glycoprotein (G) in starter cells. Subsequently cells are infected with with EnvA + RVΔG, which is trans-complemented by G to make G + RVΔG that will travel trans-synaptically to neurons providing synaptic input to starter cells. This monosynaptic spread of RVΔG is restricted because the input cells do not contain G which is required for trans-synaptic spread. In this example, starter cells are selected on the basis of Cre expression in a Cre expressing mouse line that labels a cell type of interest. In the first step (1) a helper virus that expresses TVA, G, and a marker gene (tdTomato) in a Cre-dependent manner is injected in the location of desired starter cells. This results in expression of TVA, G, and tdTomato only in the Cre+ cells (green and red) (2). After enough time for accumulation of TVA and G, EnvA + RVΔG is injected in the same location (3) and selectively infects the TVA+ starter cells. In this example the EnvA + RVΔG contains the coding sequence for GFP resulting in GFP expression in the starter cells. The RVΔG replicates in the starter cells and trans-complementation with G results in the production of G + RVΔG that moves trans-synaptically to input cells (4), which express GFP from the RV genome (green). Resulting in starter cells that are marked with both tdTomato and GFP while input cells express only GFP. Nearby neurons that do not express Cre and are not directly presynaptic to starter cells will not become labeled (light grey) (Modified from Callaway and Luo, 2015).

This modification then limits the cells that the RV can successfully infect, thereby making it a powerful tool in circuitry mapping by allowing for more discrete labeling of cells within the CNS *(*Callaway, 2008; Ugolini, 2011*)* (See Supplemental for further description).

Here, I propose that the conclusions found in previous studies were confounded by the experimental parameters and the techniques utilized and as such do not reflect a true representation of striatal spatial organization. In particular, I propose that FS cells preferentially make nearby connections to SPNs, while LTS interneurons make distant connections onto SPNs and that this difference explains the contrasting result.

To test this hypothesis, I will use a monosynaptic, retrograde rabies virus system in a transgenic mouse model to map the local input of genetically defined neurons in the striatum (Figure 11).

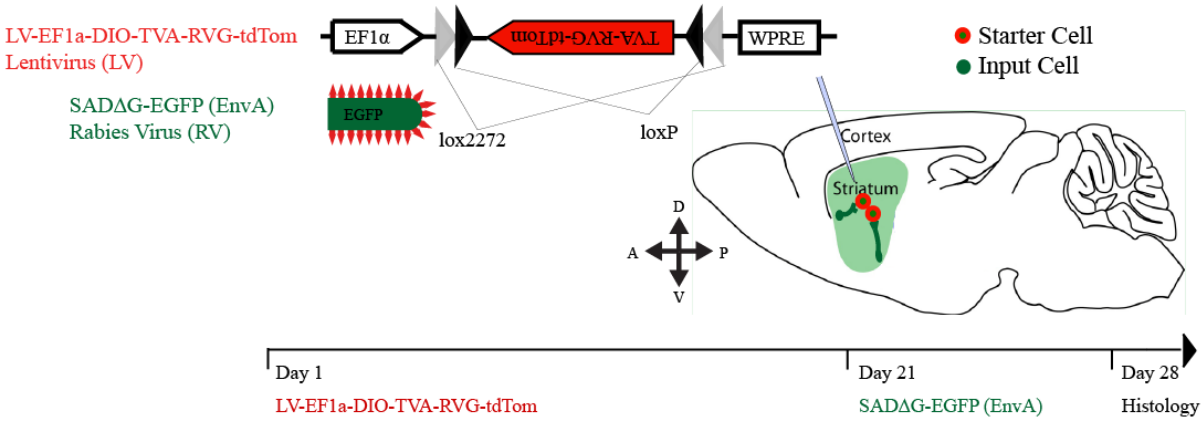


Figure 11. Rabies Monosynaptic Tracing Scheme
Cre-dependent helper virus enables pseudotyped rabies viral infection and monosynaptic spread.

Using a combination of tracing, immunohistochemistry and three-dimensional reconstruction, I expect these techniques to allow systematic mapping of the distance between GABAergic interneurons and SPNs in the striatum. I intend to use this approach to determine the average

distance of input from FS- or LTS-interneurons, respectively, onto SPNs. In addition, I will examine possible differences in this input between the two different types of SPNs, direct and indirect.

These data will provide important information about the spatial organization of local connectivity within the striatum and contribute towards a better understanding of BG circuitry.

# Chapter II

## Materials and Methods

The experimental methods and procedures performed for this thesis are described in this section. Here, we have provided the technical details for each component of the experiment and how we generated our results.

### Transgenic Mouse Lines

All procedures performed in this study have previously been approved by the Harvard Medical School Institutional Animal Care and Use Committee (IACUC) in protocol no. 03551. Experiments were performed using BAC-transgenic mouse lines that express the recombinase Cre in SPNs of the direct (Tg(Drd1-cre)EY262Gsat; from here forward referred to as "*D1-Cre*")(Gong *et al.*, 2007) or indirect pathway (B6.FVB(Cg)-Tg(Adora2a-cre)KG139Gsat/Mmucd; from here forward referred to as "*A2a-Cre*") (Shen *et al.*, 2008), thereby specifically labeling dSPNs (*D1-Cre*) or iSPNs (*A2a-Cre*), respectively.

### Identification of Cre-Positive Mice

All experiments involving animals were carried out in accordance with protocols approved by the Harvard Standing Committee on Animal Care (HCCM) following guidelines described in the US National Institutes of Health *Guide for the Care and Use of Laboratory Animals* and all efforts were made to minimize suffering. The mice were maintained at Harvard Medical School within the Warren Alpert Building barrier. The mice were housed according to HCCM guidelines and were allowed to eat and drink *ad libitum.* Mice carrying an allele that will

enable labeling of neurons by Cre from either direct (*D1-Cre*) or indirect (*A2a-Cre*) SPNs were used for all experiments. These transgenic mice were created using the BAC (bacterial artificial chromosome) method and because the number and location of BAC insertions cannot be determined, breeding BAC mice to homozygosity can cause off target unintended effects (Yang and Gong, 2005). To minimize the likelihood of interference from location or multiple copies of the BAC, all *D1-Cre* and *A2a-Cre* mice are maintained in breeding pairs with C57blk6 (wildtype) mice to produce only heterozygous or negative offspring. All mice were genotyped by PCR to confirm the presence of the transgene prior to use in all experiments. (See Supplemental).

## Viral Expression and Safety

Mice between the ages P20-P24 underwent an intracranial injection (ICI) procedure and received a volume of virus targeted to the dorsal striatum of *D1-Cre* or *A2a-Cre* mice. The mice were transferred from the standard housing barrier to the Biosafety Level 2 (BL-2) room. Both lentivirus (LV) and pseudotyped replication incompetent rabies virus (RV) are BL-2 agents. Mice that come in contact with BL-2 viruses are sequestered from the general colony and require a higher level of personal protective equipment (PPE) for the researcher.

The mice were first infected with the lentivirus, LV_EF1a_DIO (TVA-RVG-tdTom). Each brain received bilateral injections of this genetically modified LV to convey a TVA receptor to first order infected cells in a Cre-dependent manner, thereby labeling only either direct or indirect SPNs (in *D1-Cre* mice or *A2a- Cre* mice respectively). The virus was allowed to express in the brain for a period of three weeks. After this incubation period, the mice underwent a subsequent ICI and a volume of pseudotyped RV, EnvA-SADΔG-EGFP, was

injected into the same brain coordinates. The pseudotyped RV was then allowed to express for 7 days during which time the virus was only able to infect cells carrying the TVA receptor conveyed by the previous viral injection. This technique was previously established by Zampieri *et al.* (Zampieri *et al.*, 2014).

## Intracranial Injection

All lentiviral (LV) injections were performed on pre-weaned mice, ages P20-P24 and subsequent pseudotyped rabies viral injections were performed at ages P41-P45. The same procedure in its entirety was performed for both the LV and the pseudotyped RV injections. For all non-weaned pups, the total time from removal from mother to return following surgery did not exceed 120 minutes. A dedicated surgical area was scrubbed for 5 minutes with 10% Clorox followed by 70% ethanol wipe. The surgical tools were sterilized by autoclave prior to each surgical day and by bead dry sterilizer between animals on the same surgical day. Mice were taken, one or two at a time, from their home cage and placed in a small induction chamber previously filled with 2.0% isoflurane/oxygen from a standard isoflurane vaporizer with a steady oxygen flow rate of 2L/min. Upon losing consciousness, the anesthetized mouse was removed from the chamber and given an intraperitoneal (IP) injection with 5-10 mg/kg of ketoprofen as anesthetic. The mouse was then monitored for response to tail and toe pinching, if no response from the animal was observed, the surgical procedure commenced.

The animal was then transferred to the stereotaxic apparatus and a small nose cone placed over the animal's snout. The cone was connected to the outflow from the vaporizer providing a constant non-rebreathing stream 1.0-2.0% of isoflurane/oxygen mixture with a steady oxygen flow rate of 1 L/min. The nose cone was sufficiently snug around the snout to eliminate leakage

of gas. Outflow from the nose cone passed to a standard activated charcoal scavenging unit which acts to scavenge waste isoflurane. The system was entirely closed and did not permit either re-breathing by the animal or escape of isoflurane into the room. Whenever necessary, the dosage of isoflurane was adjusted on the vaporizer (approximately 1.0-2.0%) to completely eliminate both blink and pedal reflexes without causing cessation of spontaneous respiration. Once the mouse was secure on the stereotax a sterile ophthalmic, Puralube was applied to the eyes to prevent drying of the cornea.

With the animal mounted in a stereotaxic frame, the fur was shaved with an electric razor and the skin cleansed with a betadine scrub followed by a 70% ethanol wipe and this alternating process was repeated three times. The skin was then cut with a scalpel and a surgical marker was used to mark the position of the craniotomy with coordinates (in mm) 0.75 anterior and 1.75 lateral with respect to Bregma and 2.70 ventral with respect to pia. Using a hand held surgical drill, a small hole was created. A needle containing the appropriate virus was positioned above the desired coordinates and passed into the brain and small volumes (0.1-1 microliters) of virus (LV or pseudotyped RV) was injected under microprocessor control into the striatum at a rate of 50 nl/min. Once the injection was complete, a 10 minute incubation time was observed to allow for lateral diffusion of the virus into the tissue, the needle was then slowly withdrawn and the skin was sutured shut using an interrupted stitch with a 7/0 suture.

Following completion of surgery, the nose cone was removed and the animal was allowed to recover from anesthesia (approx. 5-10 minutes). During this recovery period, the animal was placed on a folded cloth towel or other compliant material on top of a heating pad ($37^{o}$C) to assist with thermoregulation. Blood, urine, etc. was removed by gentle cleaning. Direct contact with normal cage bedding was minimized because it can cause eye injuries and

respiratory and intestinal blockage in semiconscious animals. Once the animal was fully recovered from anesthesia, it was then returned to the home cage and post-operative recovery was monitored by observing locomotion and food/water intake. Ketoprofen (5-10 mg/kg) was administered twice a day for 48 hours as a post-operative analgesic.

The animals were checked after surgery and then again for seven more days after the procedure. From discussions with others using this methodology, it appears that on occasion postoperative animals (10%) appear to be in pain, evident by their tendency to remain on their bellies and move very little. This response reflects a surgical complication (e.g., bleeding) and it is recommended that animals displaying this behavior should be euthanized to minimize their discomfort. However, we did not encounter any of these complications and all the postoperative animals recovered well from surgery; they were ambulating and exploring their cages within hours after anesthetic recovery, showing no apparent irritability or ill effects.

## Intracardiac Perfusion for Tissue Harvest

An additional period of one week was allowed to pass after the RV injection, to allow for sufficient protein expression and spread of the viruses. The mice were then deeply anesthetized with pentobarbital (5 mg/body kg). The level of anesthesia was monitored to assess the righting reflex, after 3 minutes the animal was observed for the lack of a withdrawal reflex after tail pinch. Once the proper level of anesthesia was reached, the thoracic cavity of the animal was opened by midline incision using surgical scissors. A small incision was then made in the right atrium and in the left ventricle. A small gauge needle attached to silicon tubing was then inserted into the left ventricle. The animal was transcardially perfused with 10 mls phosphate buffered saline (PBS) followed by 10 mls 4% paraformaldehyde (Electron Microscopy Sciences, EM

grade, 15713-S) in 1x PBS at a rate of 5 ml/minute controlled by a peristaltic pump. The animal was then decapitated and the brain removed. The brains were then post-fixed for a period of no less than 4 hours and no greater than 48 hours, before being rinsed three times and stored in 1x PBS at 4°C. The brains were later bisected at the midline and the tissue then cut coronally into 50 μm sections using a vibratome (Leica VT 1000, Leica Microsystems, Nussloch GmbH, Germany). Each hemisphere was sliced separately and collected sequentially in 24-well plates containing pre-cooled PBS and stored at 4°C.

## Immunohistochemistry

For immunohistochemistry (IHC) the slices were stained against the presence of the parvalbumin or somatostatin proteins. This stain was performed to identify PV+ or SOM+ cells and identify PV+ or SOM+ virally labeled cells. Tissue slices were incubated in a blocking solution (6% normal goat serum (NGS) with 0.2% Triton X-100) and placed on a shaking platform for 1 hour at room temperature. The blocking solution was removed and the slices were immersed in primary antibody overnight on a shaking platform at 4°C. The primary antibodies used were anti-Parvalbumin (Millipore MAB 1572, mouse, 1:1000), anti-Somatostatin clone YC7 (Millipore MAB 354, rat monoclonal, 1:500) and anti-DarPP-32 (Novus, EP721Y, rabbit monoclonal, 1:200).

The following day the tissue was rinsed three times with PBS for 10 minutes each. The tissue then underwent a 1 hour incubation in a secondary antibody solution, mouse-Alexa-647 (Life Technologies, Goat anti-mouse IgG (H+L) Alexa Flour 647 conjugate, A-21236, 1:500), rat-Alexa-647 (Life Technologies, Goat anti-rat IgG (H+L) Alexa Flour 647 conjugate, A-21247, 1:500) or rabbit-Alexa-647 (Life Technologies, Goat anti-rabbit IgG (H+L) Alexa Flour 647, A-

21244, 1:100), in 3% NGS with 0.1% Triton X-100 at room temperature on a shaking platform. The slices were then rinsed again three times in PBS for 10 minutes each and the plates containing the tissue were returned to the shaking platform in between each rinse.

## Whole Mount Imaging

Following immuno-staining, coronal brain sections were transferred into a 20 cm dish containing PBS and using a fine paint brush, mounted in the order they were cut, from anterior to posterior, on Superfrost Plus slides (VWR, 48311-703). To reserve signal intensity, tissue slices were prevented from drying before embedding. Once each slide was complete, excess PBS was removed using a Kimwipe and Pro-Long Gold antifade, a DAPI (4',6-diamidino-2-phenylindole) containing mounting medium, (Molecular Probes, P36935) was applied to the tissue and a piece of 24 x 60 mm cover glass (Fisherbrand, 12-545-M) was gently placed on top of the slices. On average, it took about 50 to 60 consecutive 50 μm-sections to cover the entire mouse striatum. Individual sections were then imaged using a VS120 slide-imager (Olympus VS120 Whole Slide Scanner), using four channels (DAPI for morphology [blue]; mCherry to identify starter-virus transfected cells [red]; GFP for rabies transfected cells [green]; Alexa647 for PV, SOM or D-32 [magenta]).

## 3-D Reconstruction and Image Analysis

Following imaging, the data were analyzed by custom written macro that aligned the individual images, identified the positive cells in each channel and then calculated the distance between them. Despite the fact that the macro was designed to only compile and extract information based on image content, the analysis procedure was a multi-step, intensive process

that required continual manual input. To complete the acquisition, the images from one hemisphere of a brain were collected into a single folder and then loaded into the image analysis software, FIJI (Figi Is Just ImageJ) and processed through the custom macro. The macro was designed to analyze the images through the procedure explained in detail below, requiring multiple codes named ‘align1’, ‘align2’, ‘crop’, ‘measure’ and ‘ROI measure’.

The first macro, ‘align1’ generated several new components. Once loaded in, the original images were first separated by corresponding channel into 4 separate folders, T1, T2, T3 and T4 (DAPI, TRITC, FITC and CY5 respectively) and the new folder containing the images of only the DAPI channel was compressed to 1% of the original size in order to align all sections along the z-axis using the DAPI signal into a folder “T1 small”. The size of the complete set of images from this body of work totaled over 2 terabytes and the folders containing each individual set of images ranged from approximately 40 to 50 gigabytes, therefore, this compression step was necessary in order to work with files of this immense size.

Next, the ‘align2’ macro was loaded into FIJI opening a window where the minimum and maximum limits for signal threshold was defined manually which then allowed the code to continue and generate a z-stack named ‘Rigid Body Aligned’. Using the z-stack produced from ‘align2’, the image plate with the largest area of striatum anatomy was identified and the corresponding plate from the T1 folder was opened in FIJI. Using the free hand tool, the area just outside the perimeter of the striatum was traced onto the image and selected as a region of interest (ROI). This region of interest was then saved in order to be applied in the next step.

Following this, the code for ‘crop’ was loaded into FIJI and started. This step utilized the hand drawn ROI selected generated with the compressed image from ‘align2’, to designate the

corresponding area from the original image that was to be matched and aligned. The 'crop' macro then produced a z-stack of only the ROI defined area from the full sized images in folder T1. This stack was then reviewed for both proper alignment and cropping. Once confirmed the 'measure' macro was run.

In this step, cells were identified by their fluorescent signal (>2x background) in the other three channels: red only cells represent cells that received starter virus, but no rabies virus; green only cells represent cells that were rabies-transfected but did not express starter virus, these cells were monosynaptically connected to a starter cell; green and red double-positive cells represent starter cells; green and magenta double-positive cells represent cells that were monosynaptically connected to a starter cell and positive for one of the tested markers.

The 'measure' macro then generated three files, T3, T23 and T34. Each of these files was comprised of a list of ROIs that were automatically detected if they fulfilled one the parameters listed above. The T3 file contained all the ROIs detected in the green channel. The T23 file contained all the ROIs that were detected in both the red and green channels. And the T34 file contained the cells positive in the green and magenta channel. Starting with the T3 ROI file these ROIs were then all individually verified by loading the corresponding image z-stack and overlaying the ROI list. Any ROI that could not visually be confirmed as surrounding a cell in the appropriate channel was deleted from the list and the new listed saved. The T23 ROI file was then overlaid onto the corresponding image z-stack and visually confirmed. Any ROIs that did not surround a cell in the appropriate channels were deleted.

Once all of the ROIs were verified from the T3, T23 and T34 files, the 'ROI measure' macro was run. In this final step, the position for all starter cells and all monosynaptically

connected cells that were positive for the tested marker was determined and for each connected interneuron, the linear distance to its closest starter cell was calculated. This approach yielded a minimal distance between every connected FS or LTS interneuron and its closest starter cell. The program then exported all of these values into an excel spreadsheet.

## Data Analysis

Once the distance data was generated into excel files, the numbers were reviewed for data analysis. The distance values from each excel file were sorted based on target cell and genotype. Any distances that were found to be 0 were deleted as this indicated the same cell was detected as both starter and target cell. The data were analyzed using the non-parametric Mann-Whitney t-test.

## Confocal Imaging

High-resolution images of regions of interest were subsequently acquired with an Olympus FV1200 confocal microscope (Harvard Neurobiology Imaging Facility, NIH). Individual imaging planes were overlaid and projected into Z-stacks using Fiji. Confocal images represent maximum intensity projections from 50 μm confocal stacks taking with a 20x objective.

# Chapter III

## Results

The goal of this study was to establish a Cre-dependent, monosynaptic RV tracer as a method for examining local connectivity. Using this method, our intention was to characterize the spatial organization of local inputs to the principal projection neurons of the striatum, SPNs. In particular, we were interested in the distance of local GABAergic interneuron input and if the input distances from the two main classes of interneurons, FS and LTS interneurons, is different. This difference could potentially resolve the conflicting connectivity results reported from paired patch-clamp recordings and our optogenetic studies (See Introduction, Figure 8). In addition to mapping these distances, our intention was to see if dSPNs and iSPNs receive differential GABAergic input. And lastly, to examine whether the results from these previous questions reveal the average number of interneuron input, FS or LTS, to each SPN. In this section, we report our collected results for the comprehensive examination made of FS and LTS cell connectivity in the striatum.

### Optimization of Rabies Experimental Parameters

We performed experiments in both the *D1-Cre* and *A2a-Cre* transgenic lines to explore the distance of the connection in both the direct and indirect pathways. The first goal was to identify experimental conditions best suited for our questions. In particular, this would mean sparse (for optimal spatial resolution), but reliable labeling of starter cells, ideally positioned centrally in the striatum. The reported injection coordinates are the result of several rounds of optimization and used throughout all results discussed here.

In order to answer the questions put forth in our hypothesis we first had to optimize the virus regime to develop the final protocol that would be used to collect this data. The proposed method required the *in vivo* administration and expression of two highly concentrated viruses for a prolonged period of time within the striatum. In addition to determining the appropriate concentration/volume of virus to use, we also needed to ensure a sparse labeling of starter cells.

To determine optimal injection volumes, I injected 11 mice (7 *D1-Cre* and 4 *A2a-Cre*), with varying amounts of lenti and rabies virus, allowed the mice to express for the allotted period of time, carried out the IHC and examined expression levels. First, I injected 500 nl and 200 nl of starter virus and found that the lentivirus was quite toxic to the neuronal population of the striatum and in particular, was most detrimental in the immediate region of the viral injection (Figure 12).

Subsequently, I reduced the volume of lentivirus to 100 nl which appeared to have the best combination of sparsely infected cells without any visible cell death. For the subsequent injection with pseudotyped rabies virus, I made a 1:5 dilution with sterile PBS and injected 200nl. These conditions resulted in a Cre-dependent, sparse labeling of a small group of starter cells and were then utilized throughout all further experiments (Figures 13 and 14).

## Retrograde Mapping

Overall, I injected 31 mice, 19 of which were of the *A2a-Cre* line and 12 of the *D1-Cre* line. Each mouse was injected with LV and pseudotyped RV bilaterally and during tissue processing the left and right hemispheres were bisected at the corpus callosum. Each hemisphere was then processed for different antibody staining. In total, I analyzed 14 datasets for LTS-inputs (SOM labeling), 13 datasets for FS-inputs (PV labeling) and 4 datasets for lateral SPN

connections (DARPP-32 labeling). Of the 62 hemispheres of datasets produced several technical issues arose during processing which rendered some sets unquantifiable. From a total of 393 starter cells, I identified 5753 locally (i.e. within the striatum), connected/ GFP-positive cells and of those 5753 connected cells, 393 cells were positive for PV or SOM (7.4%) (Table 1). These results demonstrate that on average there are 13.6 connected cells per starter.

## Identification of Local Inputs from FS and LTS Cells

Despite using a similar number of *D1-Cre* and *A2a-Cre* mice, the number of connected GABAergic interneurons we found was much lower for iSPNs (*A2a-Cre*) than for dSPNs (*D1-Cre*), 12 vs 26 for PV and 33 vs 55 for SOM, respectively (Table 2). Since this reflects, on average, less than one connected cell per experiment for iSPNs (*A2a-Cre*), we consider the results insufficient for any statistical analysis and thus focus for our discussion on the results obtained from only the *D1-Cre* mice.

In *D1-Cre* mice, we identified 26 connected FS interneurons and 55 connected LTS interneurons. The connection distance span a large range (17.84 to 604.06 μm for FS and 25.06 to 1835.82 μm for LTS interneurons) and was significantly longer for LTS input than for FS input (123.47 +/- 25.02 μm for FS and 569.82 +/- 59.19 μm for LTS, $p < 0.0001$, Mann-Whitney t-Test) (Table 3). This difference was visibly apparent, as connected FS interneurons typically were found central in the injections site, close to starter cells and surrounded by other connected cells. In contrast, connected LTS interneurons were often found isolated from any other connected cell, suggesting that these cells indeed form connections over longer distances than any other locally connecting cells (Figure 15).

## Lateral Connections between SPNs

The majority of connected cells were neither PV positive nor SOM positive (5,360 out of 5,753 cells, 93.17%), suggesting that they are either cholinergic interneurons or laterally connecting SPNs. Identifying and distinguishing between those different input sources would allow for quantification of all GABAergic inputs to SPN so, therefore, we stained 4 doubly injected hemispheres against DARPP-32, a specific SPN marker.

Unfortunately, we encountered technical difficulties that prevented us from obtaining quantifiable results in these data sets. The antibody against DARPP-32 labeled soma and dendritic regions uniformly, whereas the SOM and PV stains were mostly confined to the cell soma. Together with the high density of SPNs in the striatum, this prevented us from identification of individual cells and made subsequent analysis impossible (Figure 16). However, confocal imaging also revealed that most GFP-positive neurons had a high density of dendritic spines, identifying them as SPN, the only cell type with high spine density in the striatum (Kawaguchi, 1996) (Figure 17). Based on these findings, we thus estimated the number of laterally connecting SPNs as the fraction of GFP-positive connected cells that were not positive for PV or SOM, respectively. This approximation revealed that 93.17% of all connected neurons in the striatum are likely SPNs and the ratio of SPN to GABAergic interneuron input is ~ 13.6:1.

In summary, the results show that connection mapping by retrograde rabies virus can be used to map local input in the striatum. This approach revealed that GABAergic interneurons account for only a fraction of all inputs and the input distance from LTS interneurons to SPNs is significantly larger than that for FS interneurons. These findings suggest that FS interneurons mediate locally restricted inhibition, whereas LTS interneurons mediate inhibition over larger areas within the striatum.

# Chapter IV

## Discussion

Further understanding of how GABAergic interneurons target other cells and how these striatal microcircuits control activity of SPNs, persists as a prominent research topic in the pursuit of understanding BG function. The difficulty in discriminating cells types and lack of any obvious structural organization within the striatum continues to impede progress in this field. The research in my thesis combines several types of emerging neuroscience tools aimed at elucidating the connectivity pattern and spatial organization of different cells types within the striatum.

My results confirm that both FS and LTS interneurons indeed make synaptic connections onto SPNs. Furthermore, they reveal a previously unknown organizational principle by demonstrating that FS interneurons preferentially make local connections onto their target cells, while LTS synapse onto cells over a much larger distance. These findings suggest different roles for these two cell types within striatal microcircuits.

After completing this body of work it was evident that we were able to answer our main question (i.e. determine the input distance of FS and LTS interneurons), but several of our additional questions remained unanswered. We were able to address the conflicting readouts from paired patch and optogenetic signaling but we were not able to collect enough data points to convincingly make statements regarding connectivity of direct versus indirect pathways, nor were we able to support our findings by identifying and quantifying SPNs via IHC. However, the results we collected do have encouraging implications in the story of striatal microcircuitry.

These findings suggest that FS interneurons mediate locally restricted inhibition, whereas LTS interneurons mediate inhibition over larger areas within the striatum.

## Technical Considerations

Several of the tools used in this study require a high degree of optimization for every individual application and as such, while this approach was a general success for testing our hypothesis, there were many technical challenges in completing this project. Using rabies as a labeling tool for mapping cellular connectivity has many facets that require a significant degree of modifications. For each new brain area where the virus is injected, the volume and concentration must be optimized not only to ensure the appropriate spread and sparse labeling, but also to assess the virus's toxicity due to concentration and length of expression.

## Pseudotyping Rabies Virus and Biosafety

The benefit of this mapping tool is carefully weighted by several limitations and risks. Creation of an accurately pseudotyped rabies virus is time consuming. Currently there is only one commercial option through which researchers can purchase the virus and this vendor is quite limited in the genetic variations and fluorophores it has to offer. This current lack of variety and options leads researchers to undertake making the virus themselves. Making these viruses not only requires a great deal of time, but also requires access to expensive equipment and the process can result in significant error if not done correctly. (Refer to Supplemental Materials).

Another significant risk stems from the safety of working with rabies viruses; they are classified as a Bio-Safety Level 2 (BL-2) agent. Working with BL-2 agents requires specific

trainings, dedicated lab spaces and equipment, as well as, a heightened level of personal protective equipment (PPE). The Center for Disease Control (CDC) defines a BL2 Agent as:

> "BSL-2 agents pose moderate hazards to personnel and the environment. It differs from BSL-1 in that: 1) laboratory personnel have specific training in handling pathogenic agents and are supervised by scientists competent in handling infectious agents and associated procedures; 2) access to the laboratory is restricted when work is being conducted; and 3) all procedures in which infectious aerosols or splashes may be created are conducted in Biosafety cabinets or other physical containment equipment."
> (Center for Disease Control, 2015).

This classification level reinforces the importance of virus specificity. The safe guards that are employed by the practice of pseudotyping and requiring a helper virus ensure that the RV is incapable of replicating on its own after injection into a host thereby limiting the possibility for the virus to infect unintended targets. Refer to Supplemental Section for a more detailed description of the pseudotyping process (Supplemental Figure 7).

## Data Set Preparation

While the methods described in this thesis were successful at answering the overall aim, there were a considerable amount of data sets that were not included in our results due to technical difficulties. The number of mice that were injected with both viruses, perfused, sliced, stained and mounted produced more than double the number of actual data sets that were successfully run through the macro and data analysis component of this project. While there were 18 data sets included in the results, there were a total of 42 data sets in total completed for this work. This is not including the mice and data sets discussed in the Supplemental section.

The variance in the number of data sets was a result of technical difficulties that arose during tissue handling. There were several types of complications encountered that left tissue unusable. First, the amount of time the tissue was allowed to remain in 4% formaldehyde, or to post-fix, greatly affected how well the tissue could be sectioned. Next, any error in mounting the tissue on the vibratome, in particular, the positioning and amount of glue used to adhere the brain tissue significantly impacted the ability to section cleanly. And lastly, during the mounting of the tissue, any air bubbles or debris that were introduced during the application of the mounting media had catastrophic effects on the ability to collect clean images of the tissue. In order for the macro to perform the 3D reconstruction of the striatum, the tissue and images had to be uniform and impeccable, thus this last challenge was the most detrimental when encountered.

When any of these issues occurred, the macro was either unable to either perform the 3D rendering or to accurately detect discrete ROIs and the data set was deemed unusable and therefore, discarded. The experimental pipeline was long and involved numerous complex manipulations in order to get the injected brain tissue successfully to the end result; advancing through all of these intricate steps to lose an entire data set because of torn slices, lint or air bubbles was an excruciating reality.

## Converging Synapses

In 2007, a review was published by Wilson suggesting that a typical SPN receives ~2000 inhibitory synapses, which suggest input from at least several hundred cells (Wilson, 2007). Interestingly, from our data we see the ratio is 13.6:1 connected cells from 450 starter cells, i.e., ~ 14 connected cells/starter cell, significantly less than expected. There are several avenues for speculation here. If we consider the estimations put forth in the Wilson review, of the ~2,000

synapses per cell identified by electron microscopy (EM), if a presynaptic cell makes on average 5 inputs to any given target cell (as a rough estimate of convergence), then they would be coming from ~400 cells, but our data indicate inputs originating from only ~14 cells. One explanation for this discrepancy is that the actual degree of convergence is much higher and any given connected cell makes multiple contacts onto a target SPN.

Additionally, my method was optimized to only label a subset of cells and therefore, we are under representing the potential pool by design. Considering that all of the cells labeled by this method are confined within a small area, it might be that we are not only getting multiple inputs from each pre-synaptic cell but we may also have labeled the same pre-synaptic cell more than once. In this instance, if the pre-synaptic cell connects to several postsynaptic targets, it is thus labeled redundantly, which would reduce the number of countable inputs. Both of the sampling factors described above would further reduce the number of detected inputs.

Our results also raise the possibility that our mapping tool was biased. Currently there are no published works to Support this theory, however, it has recently been speculated that rabies virus preferentially labels excitatory input (C.Straub and K. Huang, personal communication). Reviewing the literature, we see that the majority of groups are reporting their findings from examining excitatory connections (Wickersham *et al*., 2007; Guo *et al*., 2015; Sreenivasan *et al*., 2015). The absence of explicitly reported inhibitory connections leaves open the possibility that the virus somehow does enact a bias at the level of the synapse during infection. This bias would then result in over representation of excitatory input over inhibitory input. One last possible caveat is that our method is simply incomplete and methodologically I have only labeled a subset of cells.

## Limited Number of Identified GABAergic Connected Cells

The number of identified GABAergic connected cells was fairly limited on average and was in fact, far fewer than expected. This was surprising given that when recorded from, nearly every striatal cell (more than 90%) receives input from both FS and LTS cells, respectively (C.Straub, personal communication), suggesting not only that every SPN receives input from GABAergic interneurons, but also that every interneuron connects to several postsynaptic targets (given the much smaller number of GABAergic interneurons compared to SPNs in the striatum). Nevertheless, the number of connected interneurons identified here is such a small fraction of the starter cells, indicating that only occasionally was an interneuron labeled by the pseudotyped RV strategy. Again this lends support to the theory that this retrograde labeling is somehow ineffective, possibly due to synapse type. The body of work we set out to compile included looking for differences in the direct and indirect pathways and this may have been deterred due to this synapse preference. This possibility makes our approach very difficult; the number of animals and data sets collected was substantial in order to produce only a small sample size.

Initially we proposed to carry out a set of experiments to compare the distances between local inputs to SPNs in both the direct and indirect pathways using the *D1-Cre* and *A2a-Cre* transgenic mouse lines. After completing 11 data sets, the number of cells identified in the iSPN (*A2a-Cre)* background was substantially low and considering the number of cells that were examined (to compile this data, over 14,000 connected cells were identified) it was decided that we would not pursue results from this line and focus solely on the dSPN (*D1-Cre*) line. There is no obvious reason that we can think of to explain the why the method appeared to work better in dSPNs over that of iSPNs. To our knowledge, other than the dopaminergic input and the connection patterns, the cells of the direct (dSPNs) and indirect (iSPNs) pathways are fairly

similar. As such, it is unknown what point would bias one over the other to the extent observed. The only possibility we can suppose, is that given our very limited population of starter cells per mouse, the difference may simply have come about by chance.

## FS Make Local Connections and LTS Signal To Further Distant Targets

The results obtained here can potentially explain the difference in the results from paired patch-clamp recordings (Gittis *et al.*, 2010) and our optogenetic approach (Refer to Introduction Figure 8). Gittis *et al*. performed recordings within a 250 μm radius (maximal) and our data has mapped the distance between SPN and LTS interneuron to average 569.82 μm. The custom macros allowed us to plot and calculate a linear measurement drawn between the FS/LTS and target cells. This data set represents the average straight line distance between the two, when in actuality, these cells are highly branched and the route from interneuron to SPN is likely far more circuitous than this metric demonstrates. Therefore, the values measured here for distances between input and SPNs are likely an underestimation of their actual distance and what we have provided is the shortest distance possible.

Our method was to define the nearest connected input simply by identifying the closest neighboring cell. Another contributing factor for under representation may be that since we were working from a limited pool of starter cells, it is also possible that this is not an entirely accurate portrayal of the pattern of connectivity. Lastly, given that the average connection distance found for LTS was larger than that for FS, it also stands to reason that the underestimation for distance of the LTS connection is even greater. Together, the data obtained here strongly suggest that the difference between the results from paired recordings and optogenetic activation can be explained by the signaling distance of LTS interneurons.

## Functional Implications for Local Inhibitory Signaling

Within the striatum there are very few interneurons when compared to the total number of cells present. And while SPNs may receive inhibitory synaptic input from only a few interneurons, this input is nevertheless quite significant. A single interneuron can substantially delay the action/activity in a group of SPNs (Wilson, 2007). In addition, interneurons play important roles in neurological disorders with BG-related movement disorders (Gittis and Kreitzer, 2012) and inhibition of interneurons itself is sufficient to induce movement disorders (Gittis *et al*., 2011).

The significant differences in input length between FS and LTS interneurons raise the possibility that these two cell types have different signaling properties and hence differentially influence their target cells. It is tempting to speculate that FS interneurons mediate local, fast feed-forward inhibition (Pouille F and Scanziani, 2001) in the striatum, while LTS interneurons might mediate center-surround inhibition over a larger scale and hence contribute to spatial organization and/or preserving topographical information from cortical input. Much of the signaling effects of FS and LTS interneurons will depend on the input they receive and if this input is shared between different interneuron types and between interneurons and SPNs. As of now, this input has not been described systematically.

## Identifying Lateral Connections

The majority of connections within the striatum are comprised of lateral, GABAergic SPN-SPN circuitry (Wilson, 2007). Our initial intent was to use an antibody stain to identify what percentage of connected neurons that are not FS or LTS, but are instead laterally connected SPNs. Unfortunately the DARPP-32 (D-32) staining was not successful (Figure 16). The cells

recognized by this antibody are very abundant in the striatum and densely surrounded by processes that also stained positively and as a consequence individual cells could not be resolved reliably. It is possible that this issue could be surrounded by using confocal microscopy imaging instead of the slide scanner, but with current techniques this would require imaging time beyond realistic levels.

At this time no other marker exists that can readily be used to identify SPNs or possibly distinguish between cells of the direct (dSPNs) and indirect (iSPNs) pathways. In an effort to obtain a high definition image to demonstrate the outcome from the D-32 staining, one of these data sets were re-examined using a high magnification confocal microscope. As seen in Figure 14, most of the GFP-positive (i.e. connected) cells that are not PV or SOM-positive show a high density of dendritic spines, a hallmark of SPNs. The presence of these protrusions, therefore, strongly suggests that the majority of connected cells are SPNs forming lateral connections with other SPNs.

We found the ratio of connected SPN (5279) vs. connected interneurons (81) to be 65:1 suggesting there are 65 SPNs for every 1 FS/LTS connected interneuron. From the EM data presented by Wilson in 2007, we would expect the number of SPN inputs should be ~10-20 times greater than the input from interneurons. As our results do not reflect this ratio and instead display a strong bias towards the SPN-SPN connection, it is evident that the pseudotyped RV preferentially "prefers" this synapse type over FS/LTS-SPN synapses.

Altogether, the dynamic technological advances that have been made in the field of neuroscience not only facilitated the work within, but have answered questions and uncovered a tremendous wealth of information on how the brain functions. A major goal of this thesis project

was to have a better understanding of cellular connectivity in the striatum. These data have confirmed the LTS interneuron-SPN input, yet have left questions regarding the possibility of differential dSPN and iSPN connections. Further studies regarding this question will be required in the future and we hope that the results provided here will facilitate this. As of now, we hope that the novel organizational principle of local GABAergic inputs from FS and LTS interneurons, respectively, will contribute to the pursuit of understanding BG function and how this function is disturbed in neurological disorders.

Appendix 1

Tables

| **TABLE 1:** | **# Identified** |
|---|---|
| Starter Cells | 393 |
| Connected Cells | 5303 |
| PV+ or SOM+ interneurons | 7.8% |

| **TABLE 2:** | ***D1-Cre*** | ***A2a-Cre*** |
|---|---|---|
| Number of Mice | 12 | 19 |
| Number of PV+ interneurons | 26 | 12 |
| Number of SOM+ interneurons | 55 | 33 |

| **TABLE 3:** | **FS Cells** | **LTS Cells** |
|---|---|---|
| Number of Cells Identified | 24 | 55 |
| Distances Measured | 17.84 to 604.06 µm | 25.06 to 1835.82 µm |
| Distribution | 123.47 +/- 25.02 µm | 569.82 +/- 59.19 µm |
| p= | < 0.0001 | |

Appendix 2

Figures

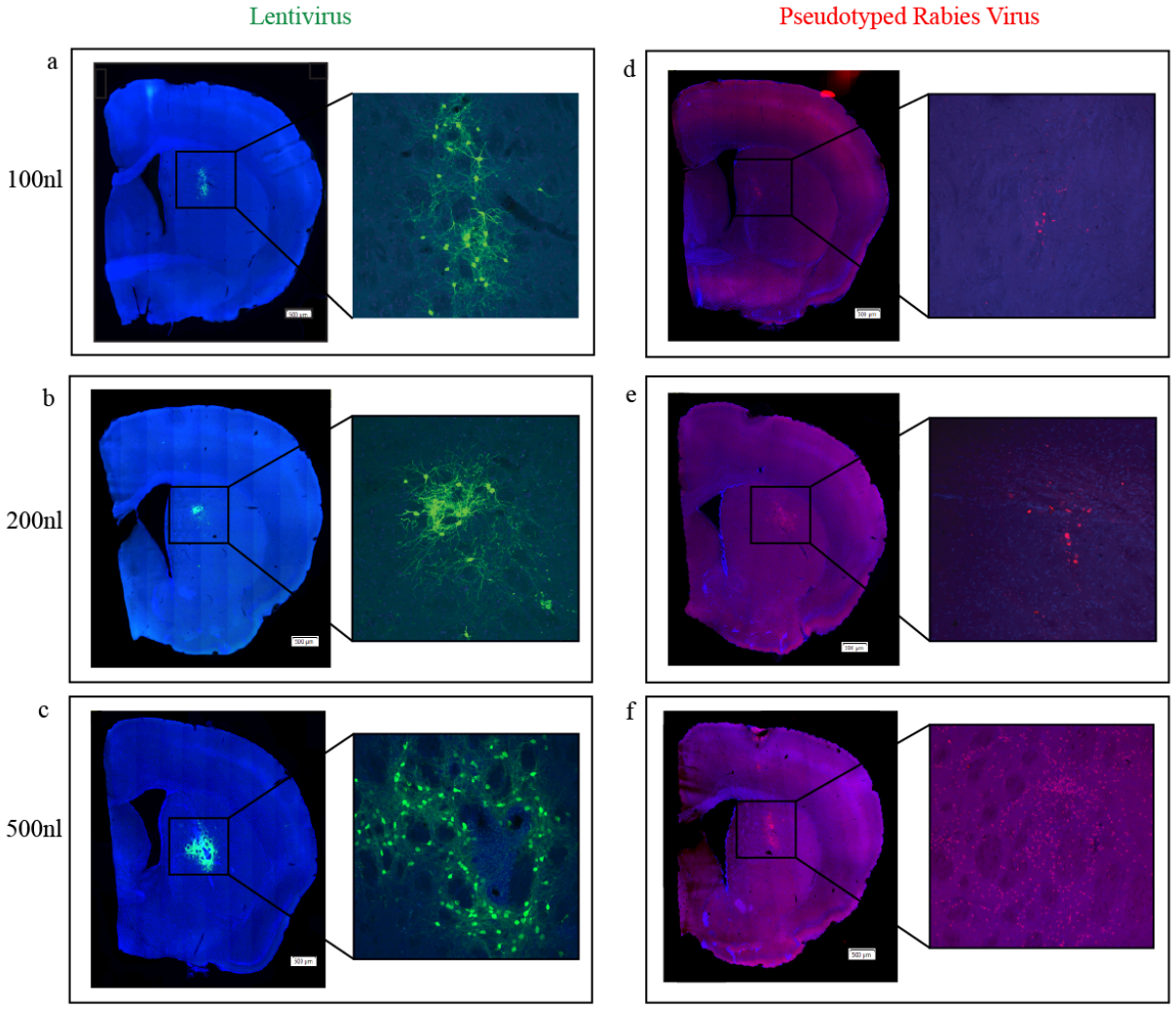


Figure 12. Optimization of LV Viral Injection Volume
Slices were mounted with DAPI mounting media (blue) and imaged for virus expression levels. Images display expression of LV (green) (a,b,c) and subsequnt pseudotyped RV (red) (c,d,e) expression.
The volume of LV was titrated in 100nl (a,c), 200nl (b,e) and 500nl (c,f). The volume of RV was held constant at 200nl of a 1:5 dilution for all trials shown. For inset images 20x high resolution confocal images were collected of the injection area for both LV and pseudotyped RV.

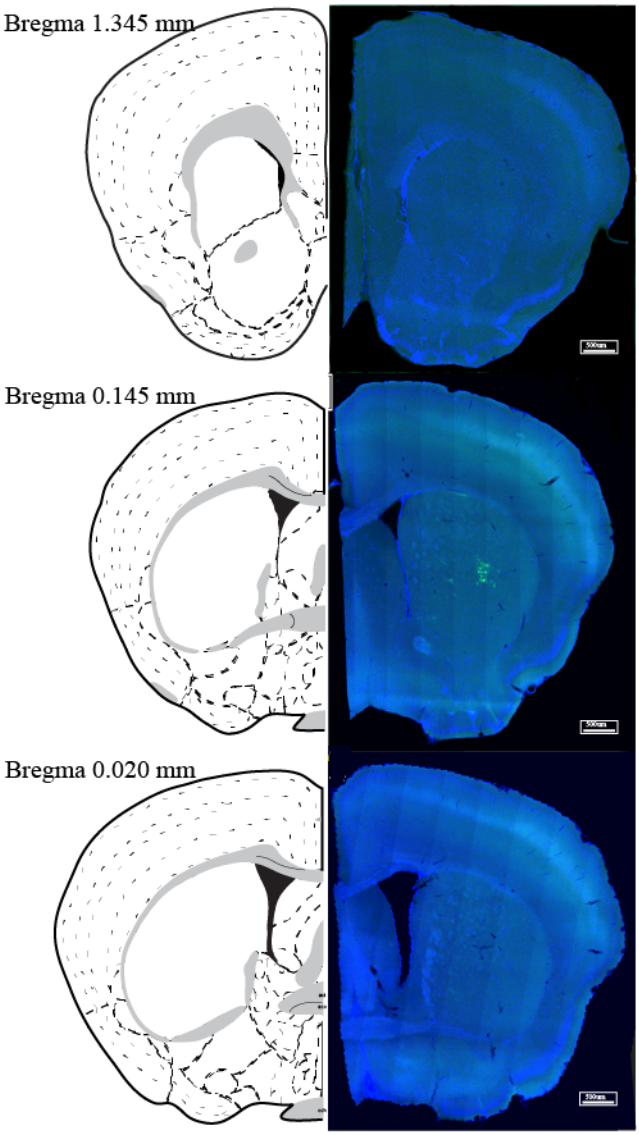


Figure 13. Striatal Injections
Visual confirmation of sparse labeling confined to the striatum.

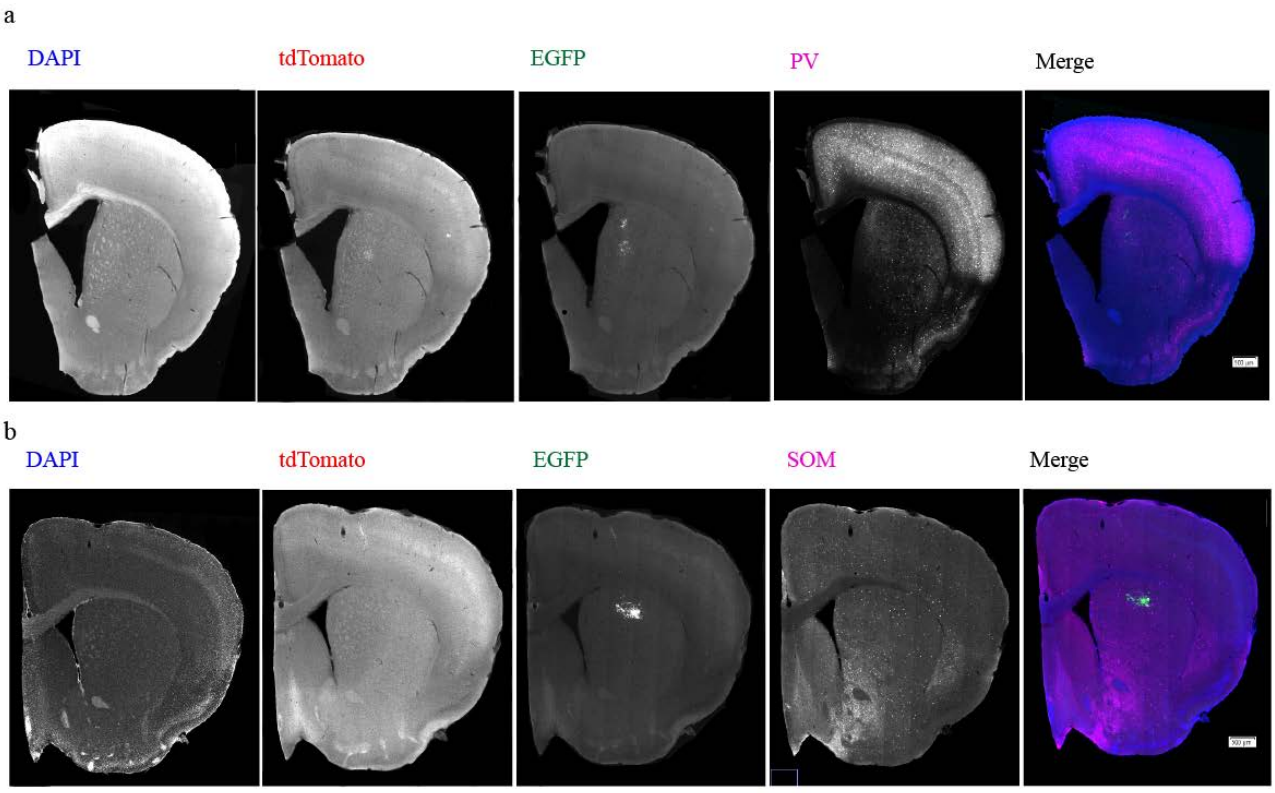


Figure 14. Four Channel Imaging
Representative images of the IHC against PV (a) and SOM (b) of the four channels isolated to show expression and the merged composite for all channels.

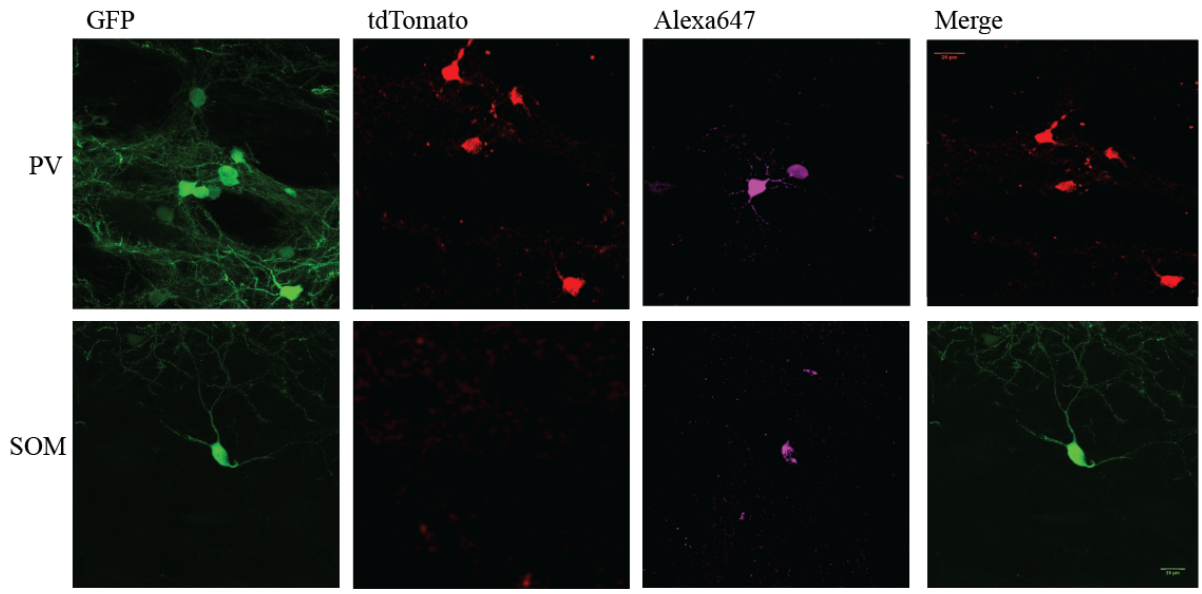


Figure 15. 20x Confocal Imaging of Target Cells
High resolution 50um z-stacks were taken on a FV1200 Confocal microscope. Images gernerated from maximun projections. Note there was no tdTomato expression found in the sample imaged in the SOM condition.

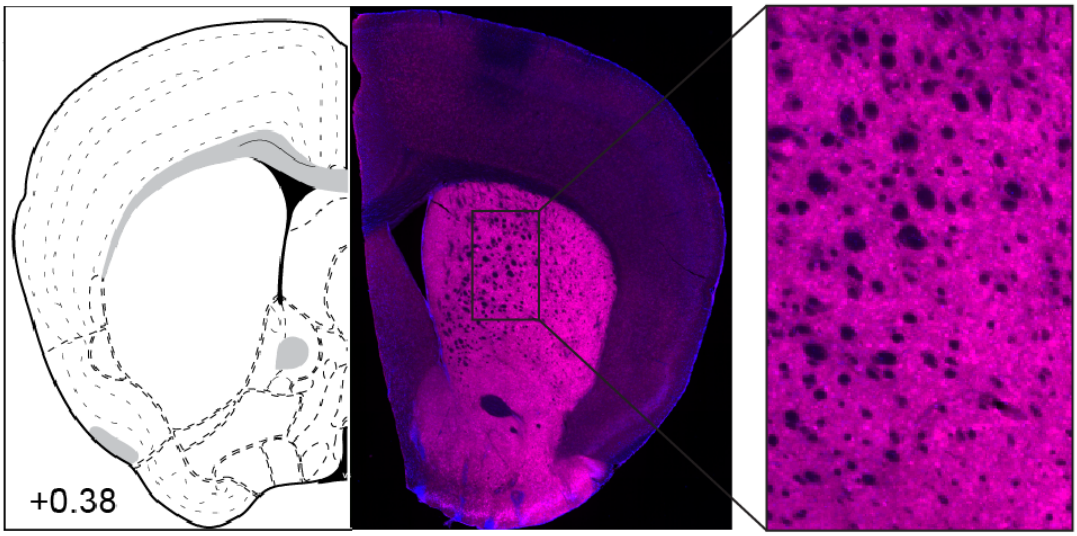


Figure 16. DARPP-32 Staining
IHC results from D-32 staining, currently the only known protein marker for SPNs. D-32 labels both the soma and dentritic regions of SPNs, the high density of this cell type in striatum make the detection of individual cell bodies difficult.

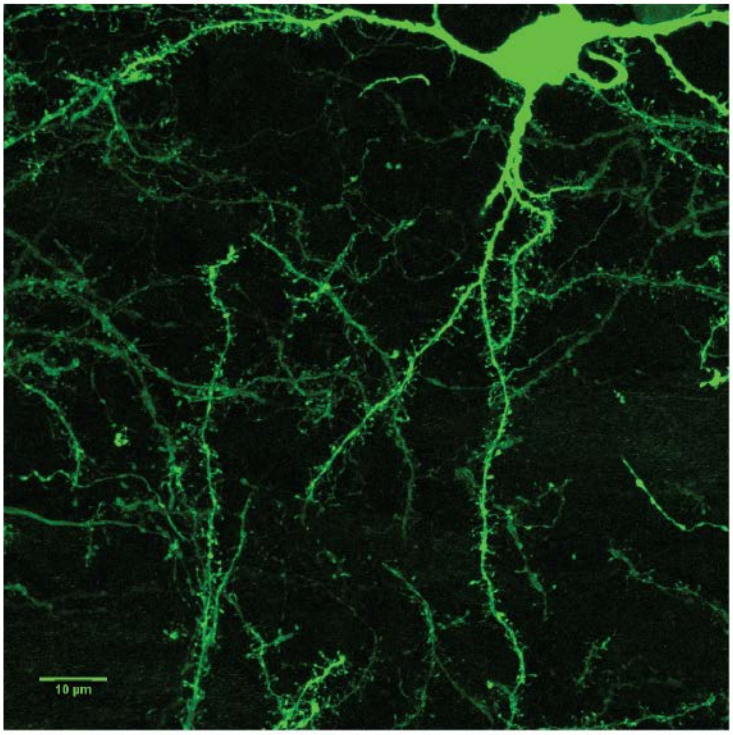


Figure 17. Spiny Projection Neuron (SPN)
~96% of the cells found in striatum are SPNs. Note the high density of dendritic protrusions called spines, which are not found on other striatal cell types.

# Appendix 3

## Supplemental Materials

### *SOM-Cre*, *PV-Cre* and *Lhx6-GFP* Reporter Lines

The development of genetically engineered mouse strains has become an invaluable tool in studying many physiological systems. The explicit labeling of individual cells types with fluorescent proteins has emerged as a common method to visual cells and monitor their behavior within living systems. With this technology, the mouse reporter model was created, in which a target gene is modified to allow monitoring of the promoter activity (Abe, 2013). The generation of an array of mouse reporter lines has enabled labeling of cellular characteristics *in vivo,* including gene expression, cell cycle progression and localization of subcellular structures (Abe, 2013).

This method was combined with the Cre/lox system to create cell-type-specific gene expression to allow mapping of neuronal circuitry and the imaging and tracking of specific cell populations (Madisen, 2010). We utilized Cre-reporter mice for the respective interneuron type, but the hypothesis presented here is built on the assumption that we have in our preliminary findings indeed recorded input from those specific interneuron classes. For this reason we validated the mouse lines carefully and also examined overlap with the marker Lhx6-GFP, which was used in the previous paired-recording study to identify striatal GABAergic interneurons.

In 1997, Kawaguchi classified several striatal cell types and reported the functional descriptions that FS interneurons specifically express PV and LTS interneurons express SOM (Kawaguchi, 1997). In recent years, several mouse lines expressing Cre under the control of the

endogenous PV or SOM promoter (IRES-Cre knock-in lines), have become available. To ensure faithful labeling of FS and LTS interneurons, respectively, in the striatum, we tested different *PV-Cre* and *SOM-Cre* mouse lines and settled on the lines developed by Silvia Arber's group for *PV-Cre* (B6;129P2-Pvalb$^{tm1(cre)Arbr/J}$) (Hippenmeyer *et al.*, 2005) and Josh Huang's group for *SOM-Cre* (Sst$^{tm2.1(cre)Zjh}$) (Taniguchi *et al*., 2011). We utilized IHC against the relevant marker and tested co-expression with genetically encoded marker that revealed expression patterns of Cre in these mouse lines (Supplemental Figure 1 and 2). While the *PV-Cre* line faithfully labeled PV-positive neurons (i.e. FS interneurons), it only labeled a subset (72.5%) of all PV-positive neurons in the striatum. In contrast, the *SOM-Cre* line labeled all SOM-positive cells, but in addition also labeled about 30% of SOM-negative cells when the reporter was expressed throughout development (Supplemental Figure 3). We believe this to reflect a transient expression of Cre in some cells early in development, since viral delivery of a Cre-reporter at P20 only labeled SOM-positive neurons (Supplemental Figure 4). Consequently, we limited all our experiments to experiments in which we expressed ChR2 in PV or SOM-positive interneurons by viral delivery during adulthood.

## Validation of the *Lhx6-GFP* Mouse Lines

The connectivity data presented by Gittis *et al.* in 2010 was performed in the *Lhx6-GFP* strain, a mouse line expressing GFP in all GABAergic interneurons (Tg(Lhx6-EGFP)BP221Gsat) (Gong *et al.*, 2003). GFP- positive interneurons were targeted for patch-clamp recordings and FS or LTS interneurons were then discriminated based on their electrical behavior (Supplemental Figure 5). To ensure that we target the same cell population as Gittis and colleagues, we further crossed our reporter lines with *Lhx6-GFP* lines and examined co-labeling.

The results confirmed a largely overlapping expression pattern (94.6% for SOM+ interneurons and 72.5% for PV+ interneurons) (Supplemental Figure 6).

Altogether these experiments demonstrate that our approach not only faithfully examines connectivity from FS and LTS interneurons onto SPNs, but also confirms that we targeted our optogenetic recordings toward the same cell population that Gittis *et al*. examined using the paired recordings approach. Hence the differences in the outcome are not due to examining different cell types, but must be due to these reasons and the hypothesis put forward here addresses this difference.

## Discovery of Non-Pseudotyped Rabies Virus

When we began this the work described in this thesis, our preliminary tests were aimed to determine the appropriate concentration and volume of virus to inject into the striatum for optimal sparse expression. At the time our lab had been gifted a supply of RV that was used in these initial experiments. Eight mice (3: *D1-Cre* and 5: *A2a-Cre*) were injected with different volumes of LV_EF1a_DIO(TVA-RVG-tdTom) followed three weeks later by an injection of SADΔG(EnvA)-EGFP* (* used to denote the difference between this variant and the accurately pseudotyped SADΔG(EnvA)-EGFP virus that was eventually used to produce the data in this thesis). One week after the second injection the mice were sectioned and the tissue scanned for presence and spread of viral expression.

While examining the hemispheres from different volumes of injected LV (500 nl, 200 nl, 100 nl and 50 nl), the degree of spread and number of cells infected with the RV appeared suspicious. The spread and number of green cells did not appear to be confined to the area of the

injection coordinates nor did the number of green cells appear to decrease appropriately based on the titrated amount of LV injected. The infection pattern of the RV led us to believe that this virus was capable of infecting cells that did not contain the TVA receptor. In order to answer this question a number of controls were performed.

Our first control was to perform an *in vitro* test of the SADΔG(EnvA)-EGFP* virus in Human Embryonic Kidney cells (HEK293). Without the initial infection of LV_EF1a_DIO(TVA-RVG-tdTom) to convey the TVA receptor for the EnvA coat protein to cells, the RV should not be expressed (Supplemental Figure 7). When added to HEK293 cells, we found the SADΔG(EnvA)-EGFP* virus was in fact expressed, indicating that the virus was incorrectly or incompletely pseudotyped during production. To confirm this *in vivo*, the virus was injected by itself into the striatum of both wild-type and *D1-Cre* mice. The virus was allowed to express for one week before the tissue was sectioned and scanned. In both instances we observed green cells; the SADΔG(EnvA)-EGFP* virus was able to infect cells without the inclusion of the helper virus. This expression in the controls meant that the RV was not confined to the Cre positive cell population in our initial experiments. Not only was this discovery important because the virus would have undermined the entire strategy of this project, but non pseudotyped RV carries with it a higher level of biosafety concerns and we were unknowingly using a highly infectious agent with only the protection procedures for the pseudotyped variant.

After this discovery our lab began producing pseudotyped RV in house and performed both of the control experiments above to demonstrate the pseudotyping was done correctly prior to releasing the RV for experiments.

## Genotyping of *D1-Cre* and *A2a-Cre* Transgenic Mice

Tail DNA collected from each mouse was digested and tested for the presence of the correct transgene. At the time of collection each tail was placed into a separate well in a 96-well block. To each well, 300 µl of 20 mg/ml of Proteinase K/Direct PCR mixture was added making sure that the tissue was submerged in the liquid. The 96-well block was then covered securely with an adhesive lid and placed at 55$^{o}$ overnight. The following morning, 200 µl of lysate was removed from each well and transferred to PCR tubes. The lysate mixture was then placed into a thermocycler and run at 85$^{o}$ for 45 minutes in order to deactivate the Proteinase K. The DNA product was then ready to use in the PCR reaction. The PCR reaction was set up following the recipe in Table 1, using Generic Cre primers for both mouse lines; the primers as well as the PCR program are listed below (Supplemental Table 2 and 3). PCR products were run on a 2% agarose gel for 25 minutes at 110V to resolve the bands. Mice were selected as Cre-positive based on the presence or lack of a band at 100 base pairs (bp) (Supplemental Figure 8).

Appendix 4

Supplemental Tables

| Table 1. PCR Recipe | | Volume/ Reaction (µl) |
|---|---|---|
| 1 | 10 mM Forward Primer | 1 |
| 2 | 10 mM Reverse Primer | 1 |
| 3 | Tail DNA | 2 |
| 4 | Nuclease-free water | 9.5 |
| 5 | 2x GoTaq Green Mastermix | 12.5 |
| | Total Reaction | 26 |

| Table 2. Primers | Primer Name | Sequence | Product Size (bp) |
|---|---|---|---|
| Generic Cre | oIMR1084_F | 5'-GCGGTCTGGCAGTAAAAACTATC-3' | 100 |
| | oIMR1085_R | 3'-GTGAAACAGCATTGCTGTCACTT-5' | |

| Table 3. PCR Program LOWE1 | | |
|---|---|---|
| Step | Temperature | Time (min) |
| 1 | 95˚ C | 5:00 |
| 2 | 95˚ C | 0:30 |
| 3 | 53˚ C | 0:30 |
| 4 | 72˚ C | 1:00 |
| 5 | Go to 2, repeat 34x | |
| 6 | 72˚ C | 5:00 |
| 7 | 4˚ C | Forever |

Appendix 5

Supplemental Figures

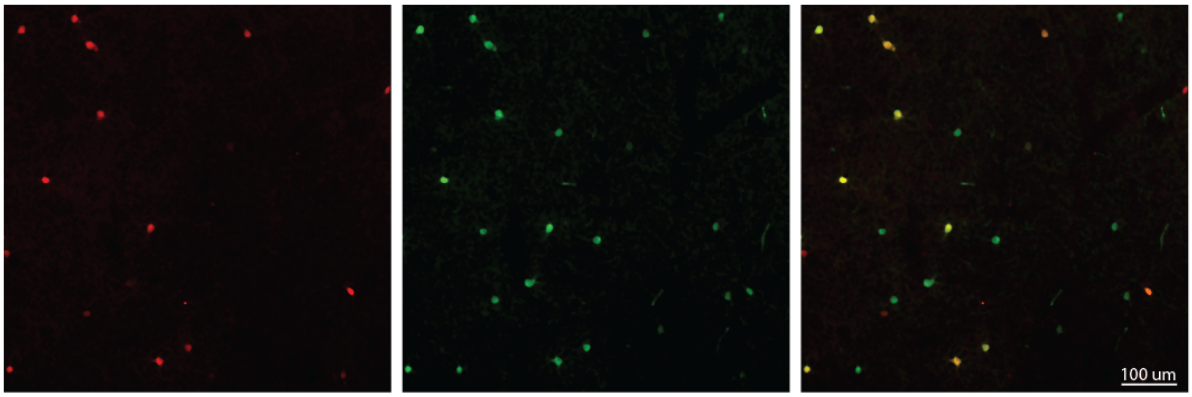


Supplement Figure 1. Validation of PV Labeling
*PV-Cre* Mouse crossed with a tdTomato strain to produce a *PV-Cre* reporter line that labels PV+ cells red (a). IHC against PV (b) and the merge of both images (c). 95.1% of all *PV-Cre* positive cells were also PV-positive by Immunohistochemistry, but only ~73% of all PV-postive cells were Cre-expressing indicating PV cells are labeled faithfully but without complete penetrance.

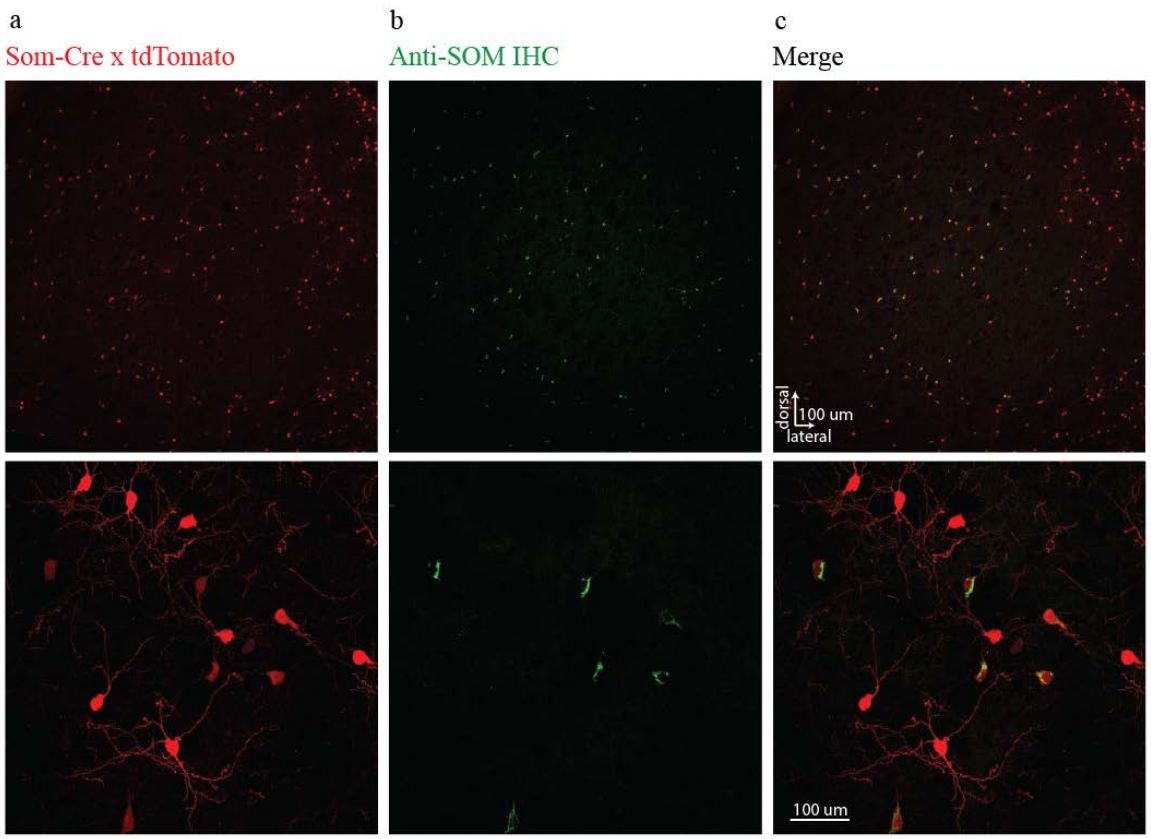


Supplement Figure 2. Validation of SOM Labeling
*SOM-Cre* Mouse crossed with a tdTomato strain generating a *SOM-Cre* reporter mouse that labels SOM+ cells red (left panels). IHC against SOM (middle panels). The merged images (right panels) indicate that early in development there are ~30% of SOM-negative cells also labeled by this reporter.

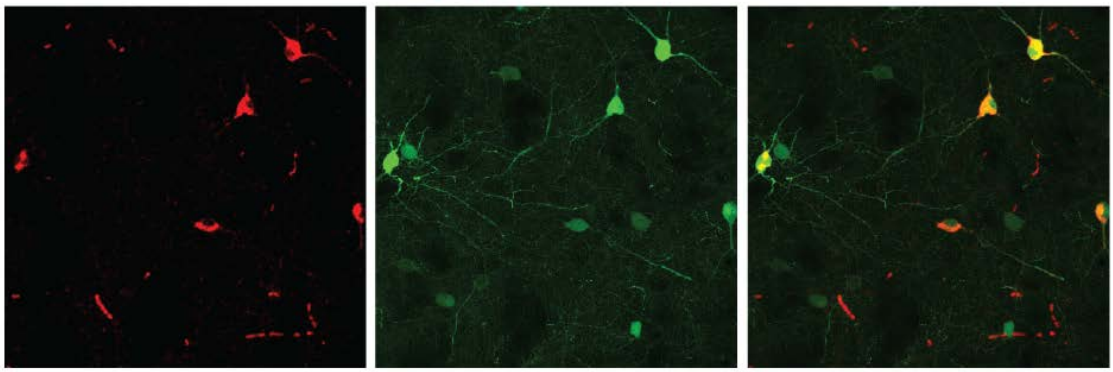


Supplement Figure 3. Confirmation of Target Cell Labeling
Using IHC we were able to confirm that 94.6% for all SOM positive cells were also Lhx6-GFP positive.

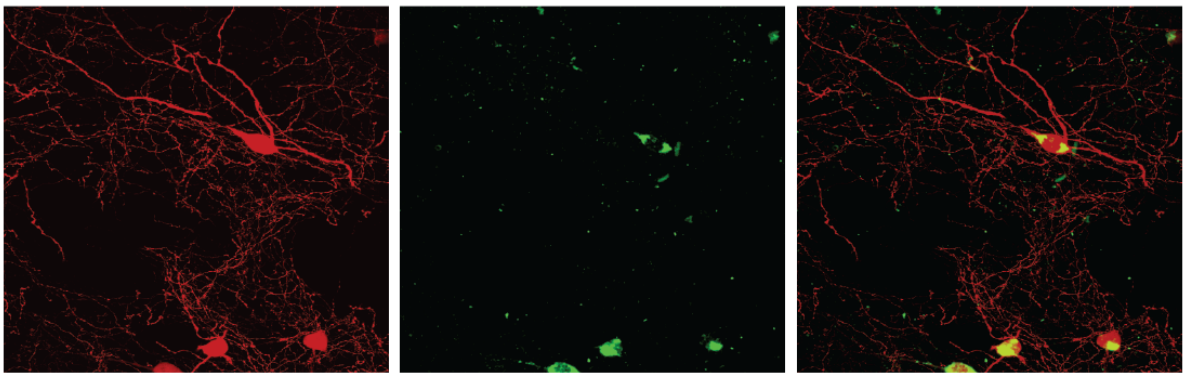


Supplement Figure 4. Cre Expression During Development
Cre reporter virus injected at P20 reveals only SOM+ cells were infected (left), as was confirmed by IHC (middle), the overlap of these images demonstrates the transient expression of Cre in SOM-negative cells is shut off during development (c).

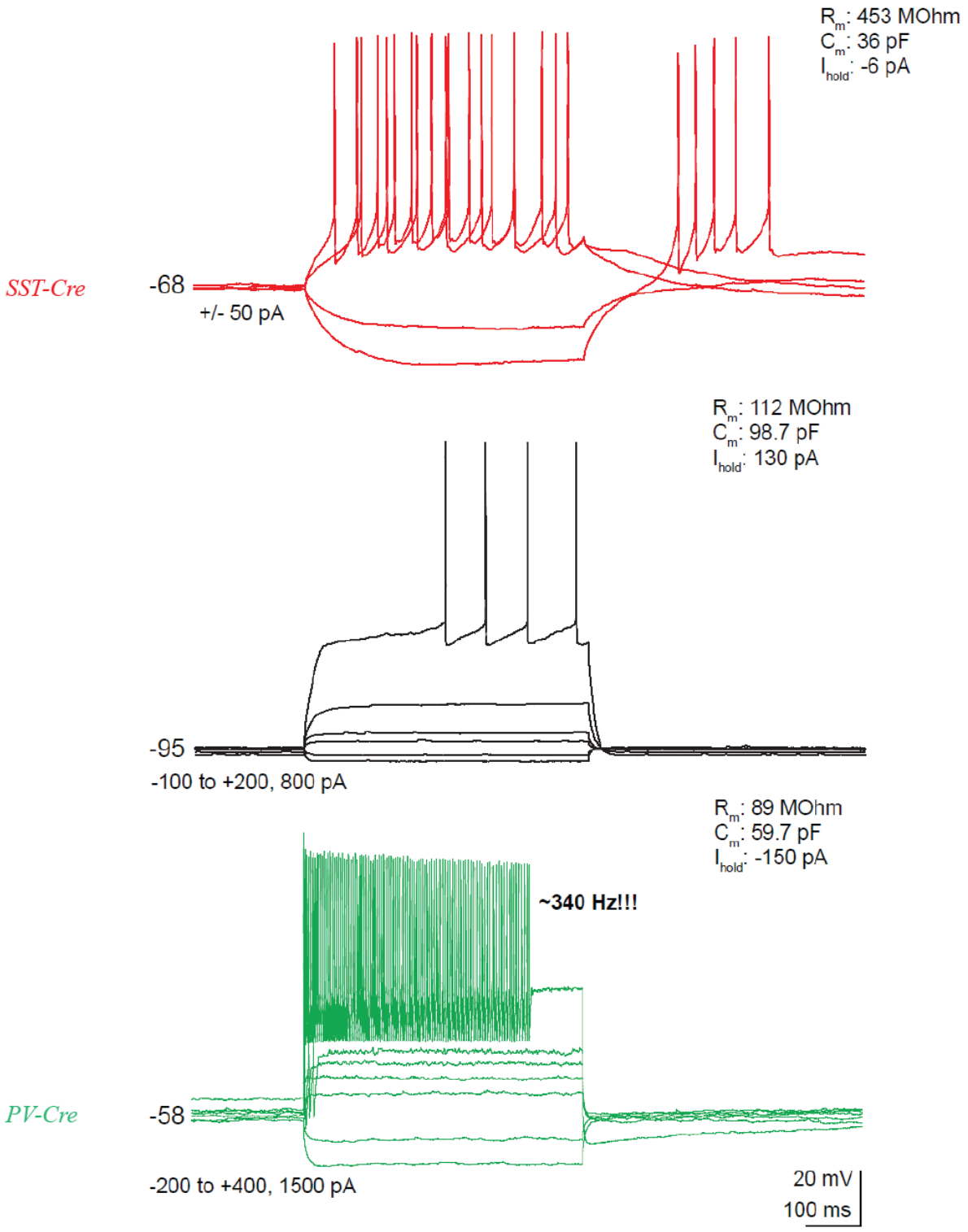


Supplement Figure 5. Patch-Clamp Recording of Targeted Cell Types
SOM- and PV-positive cells behave electrically similar to FS and LTS interneurons, respectively, as described by Kawaguchi.

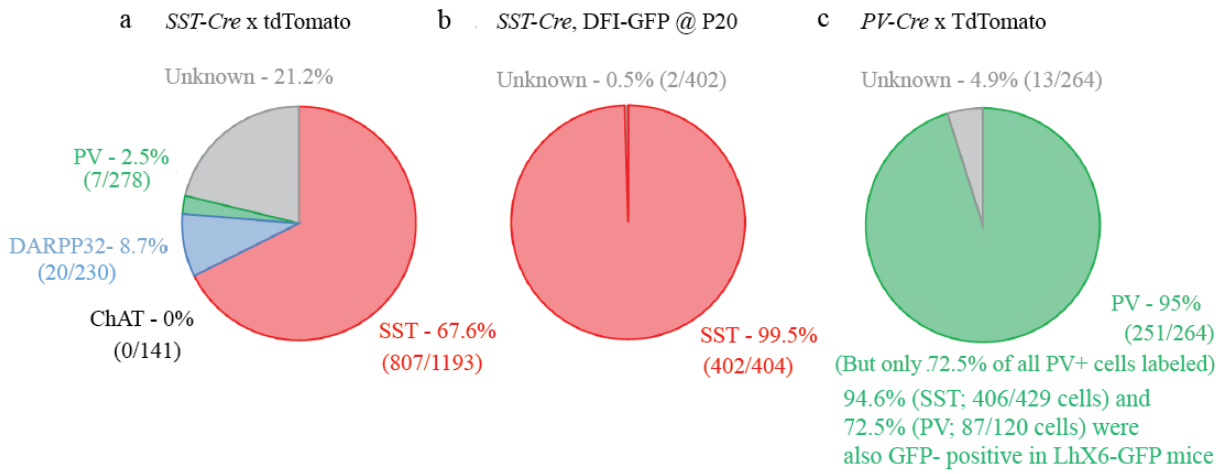


Supplement Figure 6. *SOM-Cre* and *PV-Cre* Mouse Line Validation
Summary stastics showing expression patterns of labeled SOM+ and PV+ cells identified by IHC (a,c) and viral infection during adulthood (b).

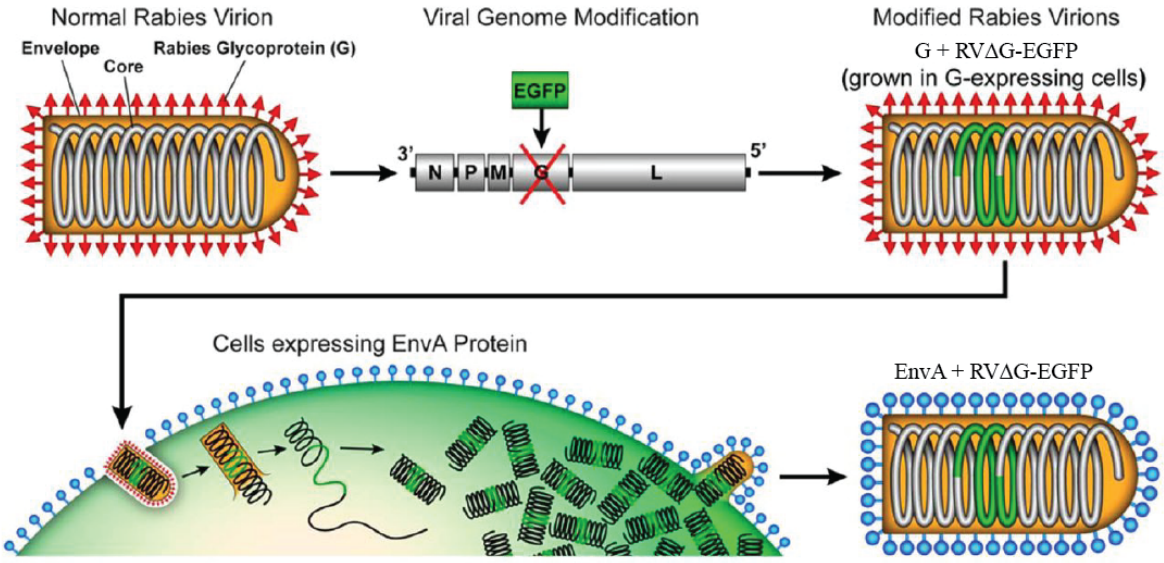


Supplement Figure 7. Glycoprotein Deletion and EnvA Pseudotyping of Rabies Virus
Normal rabies viral particles (top, left) consist of a viral core surrounded by a host cell-derived membrane envelope where the rabies glycoprotein (G; red spikes) is embedded. The core of the virus consists of structural proteins and the negatively charged RNA genome. The genome codes for five different proteins, including G (top, middle). The viral genome can be modified so that the coding sequence for G is removed and replaced with the coding sequence for a transgene, such as tdTom, which will be expressed in infected cells. G-deleted rabies virus particles (RVΔG) are initially produced *de novo* from DNA and then can be propagated indefinitely (Osakada and Callaway, 2013). When propagated in cells that express G (not shown), these RVΔG particles will then bud out from the host cells with G on their envelope (G + RVΔG, top, right). RVΔG particles that emerge will then have EnvA on their envelope (bottom, right) and can be called pseudotyped. These EnvA-pseudotyped particles are designated EnvA + RVΔG (Modified from Callaway and Luo, 2015).

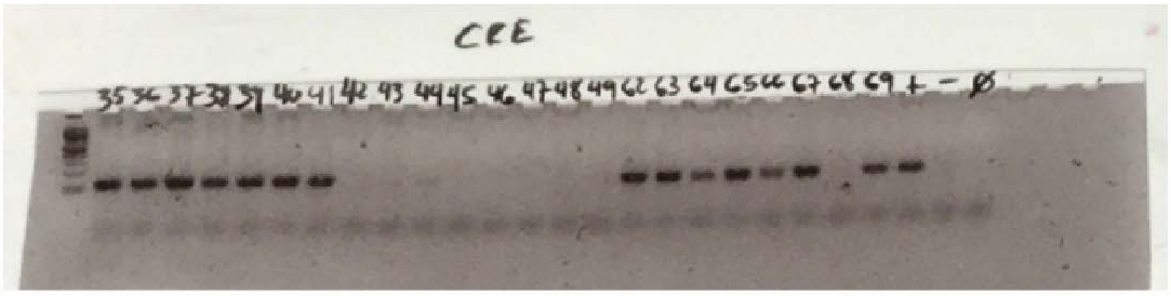


Figure 8. Example of Cre Genotyping
Results shown here demonstrating positive and negative results from mice numbers 35-49, 62-69 followed by positive, negative and no DNA controls.

List of Abbreviations

BAC – Bacterial Artificial Chromosome

BG – Basal Ganglia

BL2 – BioSafety Level 2

ChAT – Choline O-Acetyltransferase

ChR2 – Channel Rhodopsin

CINs – Cholinergic Interneurons

CNS – Central Nervous System

dSPNs – Direct Spiny Projection Neurons

DarPP32 (D-32) – Dopamine- and cAMP-regulated neuronal phosphoprotein, kDa

DAPI – 4',6-diamidino-2-phenylindole

EM – Electron Microscopy

FIJI – Fiji Is Just Image J

FS – Fast-Spiking Interneurons

GABA – Gamma-Aminobutyric acid

GC/ML – Genome Copies per milliliter

GP – Globus Pallidus

GPe – Globus Pallidus external compartment

GPCR – G protein coupled receptor

HEK293 – Human Embryonic Kidney Cells

ICI – Intracranial Injection

IHC – Immunohistochemistry

IP – Intraperitoneal

iSPNs – Indirect Spiny Projection Neurons

IU/ML – Infectious Unit per milliliter

LTS – Low-Threshold-Spiking Interneurons

LV – Lentivirus

NGS – Normal Goat Serum

NT – Neurotransmitter

PBS – Phosphate Buffered Saline

PPE – Personal Protective Equipment

PV – Parvalbumin

PV+ – Parvalbumin Positive

ROI – Region of Interest

RV – Rabies Virus

SNr – Substantia Nigra Pars Reticulata

SOM – Somatostatin

SOM+ (SST+) – Somatostatin Positive

SPNs – Spiny Projection Neurons

STN – Subthalamic Nucleus

TVA – Avian Tumor Virus Receptor A

## Definition of Terms

Acetylcholine – The first neurotransmitter discovered one of many in the autonomic nervous system. It acts on both the peripheral nervous system and central nervous system and is the only neurotransmitter used in the motor division of the somatic nervous system. It is also the principal neurotransmitter in all autonomic ganglia.

Action Potential – The change in electrical potential associated with the passage of an impulse along the membranes of a cell.

Arborization – Elaborate branching structures at the end of neurons.

Aspiny Neuron – Striatal cells with smooth dendrites and short axons that are confined to the caudate nucleus or putamen. These cells secrete GABA, neuropeptide Y, somatostatin, or some combination of these.

Bacterial Artificial Chromosome (BAC) – Large-insert DNA clones based on the *Escherichia coli* Fertility factor. The structural features of the F-factor allow stable maintenance of the individual human DNA clones, as well as, easy manipulation of the cloned DNA.

Basal Ganglia – A set of subcortical structures that interact with the cerebral cortex to regulate motor, cognitive and affective function through reinforcement learning and action selection. Its input structure, the striatum, receives a dense dopaminergic input that is critical for reinforcement learning and whose dysfunction contributes to motor and cognitive pathologies.

Cation – Any positively charged atom or group of atoms.

Cortex – The outer layer of the cerebrum with neurons in various layers that connect vertically to form small microcircuits.

Cre Recombinase – A tyrosine recombinase enzyme derived from the P1 Bacteriophage. The enzyme uses a topoisomerase I like mechanism to carry out site specific recombination events. The enzyme's unique and specific recombination system is exploited to manipulate genes and chromosomes in a huge range of research applications.

DAPI – A fluorescent stain that binds strongly to A-T rich regions in DNA. It is used extensively in fluorescence microscopy as a nuclear stain.

Dendrite – A short branched extension of a neuron along which impulses received from other cells at synapses are transmitted to the cell body.

Dendritic Spine – A small protrusion from a neuron's dendrite that typically receives input from a single synapse of an axon.

Direct pathway (D1) – A neuronal circuit within the central nervous system through the basal ganglia which facilitates the initiation and execution of voluntary movement.

Dopamine – The immediate precursor of noradrenaline in the body, found especially in nervous and peripheral tissue and formed by decarboxylation of dopa; 3,4-dihydroxyphenylethylamine, C8H11NO2.

Electrophysiology – The measurement and characterization of the electrical properties of cells and tissues, particularly neurons and neuronal tissue.

Excitability – A property of a cell, allowing it to respond to stimulation by rapid changes in membrane potential produced by ion fluxes across the plasma membrane. This is most

commonly associated with neurons but more recently astrocytes have also been shown to exhibit 'cellular excitability', resulting from changes in calcium ion concentration in the cytosol.

Feed-Forward Inhibition – A signaling pattern in which a presynaptic cell excites an inhibitory interneuron that subsequently inhibits another cell. A way of shutting down or limiting excitation in a downstream neuron in a circuit.

Fluorescence Imaging – The visualization of fluorescent dyes or proteins as labels for molecular processes or structures. It enables a wide range of experimental observations including the location and dynamics of gene expression, protein expression and molecular interactions in cells and tissues.

Fluorescent Labelling – The process of covalently binding fluorescent dyes to biomolecules such as nucleic acids or proteins so that they can be visualized by fluorescence imaging.

Fluorescent Proteins – Fluorescent proteins are proteins that absorb light and re-emit it at a longer wavelength. They can be genetically encoded as fusions to other proteins to act as labels.

Fluorophores – A chemical molecule that can emits light immediately upon excitation.

Gamma-Aminobutyric acid (GABA) – The chief inhibitory neurotransmitter in the mammalian central nervous system; plays the principle role in reducing neuronal excitability throughout the nervous system.

GABAergic Interneurons – Inhibitory interneurons of the central nervous system.

Genotype – The genetic makeup of a cell, organism or individual with reference to a particular characteristic. In diploid or polyploid individuals, it refers to what combination of alleles the individual carries.

Genotyping – A form of genetic analysis that determine DNA sequence at sites of variation in a diploid genomic complement.

Globus pallidus – The smaller, medial part of the lenticular nucleus of the brain, which is paler than the adjacent putamen and consists of two segments. Also called pallidum.

GPCR – G protein coupled receptor, seven-transmembrane domain receptors that respond to external stimuli to modulate signal transduction and other cellular responses.

Glutamatergic – Referring to a chemical agent whose function is to directly modulate the excitatory amino acid system.

HEK293 Cells – Human embryonic kidney cell derived cell line.

Hierarchical connectivity – The concept that one class of neurons is functionally downstream from another. The two classes may be in separate areas or locally intermingled. This feedforward arrangement implies control of the downstream population by the upstream population.

Histology – The study of the microscopic anatomy or structure of tissues.

Heterozygote – Having two different alleles of a particular gene or genes and so giving rise to varying offspring.

Homozygous – A cell is said to be homozygous for a particular gene when identical alleles of the gene are present on both homologous chromosomes.

Huntington's disease – An inherited neurodegenerative condition in which neurons break down over time affecting muscle coordination and leading to significant mental decline.

Immunohistochemistry – A technique for detecting molecules of interest within tissues using antibodies. Probes or enzymes conjugated to primary antibodies that bind the target molecule (or secondary antibodies that recognize the primary antibody) report the location of targets in tissue or cell samples for imaging.

*in vitro* – Studies performed with cells or biological molecules outside their normal biological context.

*in vivo* – Studies performed with cells or biological molecules within their normal biological context.

Indirect Pathway (D2) – A neuronal circuit through the basal ganglia and several associated nuclei within the central nervous system which helps to prevent unwanted muscle contractions from competing with voluntary movements.

Interneuron – Also called local circuit neurons, neurons that form a connection between other neurons; they are neither motor nor sensory. Referring to neurons whose axons connect only with nearby neurons.

Lateral Inhibition – The capacity of an excited neuron to reduce the activity of its neighbors by disabling the spread of action potentials from excited neurons to neighboring neurons in the lateral direction.

Lenti Virus – Any member of a group (now the genus Lentivirus) of non-oncogenic retroviruses which includes the viruses responsible for certain slow virus diseases (such as visna and maedi in sheep, equine infectious anemia and caprine arthritis-encephalitis) and the human, simian, feline and bovine immunodeficiency viruses.

Medium Spiny Neurons (MSNs) – Also known as Spiny Projection Neurons (SPNs), a special type of GABAergic inhibitory cell representing 90-95% of the neurons within the striatum of the basal ganglia.

Monosynaptic – Involving a single synapse.

Movement Disorders – A group of neurological syndromes in which the hallmark symptom is paucity of movement, excessive and/or involuntary movement or tremor. Movement disorders can be neurodegenerative, such as Parkinson's disease and Huntington's disease, but they can also be induced by medication, infection, inflammation or trauma.

Neurotransmitter – Endogenous chemicals that transfer signals across a synapse or junction from one neuron to a target cell.

Optogenetics – A method that uses light to modulate molecular events in a targeted manner in living cells or organisms. It relies on the use of genetically-encoded proteins that change conformation in the presence of light to alter cell behavior, for example, by changing the membrane voltage potential of excitable cells.

Parkinson’s disease – A degenerative disorder in the CNS that affects motor control that arises from the death of dopamine producing neurons in the substantia nigra.

Parvalbumin – A calcium binding muscle protein of low molecular weight found in some vertebrates.

Patch clamp – A laboratory technique in electrophysiology that allows the study of single or multiple ion channels in cells.

Pentobarbital – A fast acting barbiturate that causes death by respiratory arrest.

Pseudotyped – Phenotypic altering in retroviruses that results in a genome from a parent containing a defective envelope housed inside the protein coat from a helper virus.

Principle Projection Cells – Also known as Medium Spiny Neurons or Spiny Projection Neurons. A GABAergic inhibitory cell comprising ~90-95% of all neurons within the striatum.

Projection Cells – Neurons who axons project to distant regions of the brain or spinal cord.

Polymerase Chain Reaction (PCR) – A technology in molecular biology in which a single or few copies of a piece of DNA are amplified across several orders of magnitude, generating thousands to millions of copies of a particular DNA sequence.

Replication Incompetent – Viral vectors are a tool commonly used by molecular biologists to deliver genetic material into other cells. However, at times this can involve the deletion of a part of the viral genome critical for viral replication. Such a virus can efficiently infect cells but once the infection has taken place, requires a helper virus to provide the missing proteins for production of new virion (for subsequent cell infection).

Retrograde – To travel in an upstream direction opposite to the movement of something else.

Stereotax – Referring to surgical techniques for scientific investigation that permit the accurate position of probes inside the brain based on three-dimensional diagrams.

Striatum – The neostriatum or striate nucleus is a subcortical part of the forebrain. It is the major input station of the basal ganglia system.

Soma – Cell body or bulbous end of a neuron.

Somatostatin – A hormone that is widely distributed throughout the body and acts as an important regulator of nervous system function by inhibiting the secretion of other hormones.

Substantia nigra – A large nucleus of the midbrain that contains (especially in adult humans) a layer of dark melanin-laden cells and is a part of the extrapyramidal motor system which is involved in Parkinson's disease and certain other disorders of movement.

Synaptic Transmission – The process by which signaling molecules called neurotransmitters are released by a neuron and bind to and activate the receptors of another neuron.

Synapse – A structure that permits a neuron to pass an electrical or chemical signal to another cell.

Transgenic Mice – Mice that contain additional foreign DNA in every or a subset of cells that allow them to be used as a tool to study gene function or regulation, often used to model human diseases.

Viral tracing – A method that uses viral movement between cells as a label to determine the cells' connectivity. Viruses are most commonly used as tracers to define neural circuitry.

3-D Reconstruction – The process of generating a computer model of the 3D (3-dimensional) appearance of an object from a set of two-dimensional images.

References


Abe, T. and Fujimori, T. (2013). Reporter Mouse Lines for Fluorescence Imaging. Develop. Growth Differ. *55*, 390–405.

Ade, K.K., Wan, Y., Chen, M., Gloss, B. and Calakos, N. (2011). An Improved BAC Transgenic Fluorescent Reporter Line for Sensitive and Specific Identification of Striatonigral Medium Spiny Neurons. Front Syst Neurosci *5*.

Albin, R.L., Young, A.B. and Penney, J.B. (1989). The functional anatomy of basal ganglia disorders. Trends in Neurosciences *12*, 366–375.

Albin, R.L., Young, A.B. and Penney, J.B. (1995). The functional anatomy of disorders of the basal ganglia. Trends in Neurosciences *18*, 63–64.

Alexander, G.E. and Crutcher, M.D. (1990). Functional architecture of basal ganglia circuits: neural substrates of parallel processing. Trends in Neurosciences *13*, 266–271.

Aosaki, T., Kimura, M. and Graybiel, A.M. (1995). Temporal and spatial characteristics of tonically active neurons of the primate's striatum. Journal of Neurophysiology *73*, 1234–1252.

Bamford, N.S., Zhang, H., Schmitz, Y., Wu, N.-P., Cepeda, C., Levine, M.S., Schmauss, C., Zakharenko, S.S., Zablow, L. and Sulzer, D. (2004). Heterosynaptic Dopamine Neurotransmission Selects Sets of Corticostriatal Terminals. Neuron *42*, 653–663.

Beatty, J.A., Sullivan, M.A., Morikawa, H. and Wilson, C.J. (2012). Complex autonomous firing patterns of striatal low-threshold spike interneurons. J Neurophysiol *108*, 771–781.

Bennett, B.D. and Bolam, J.P. (1994). Synaptic input and output of parvalbumin-immunoreactive neurons in the neostriatum of the rat. Neuroscience *62*, 707–719.

Bevan, M.D., Booth, P.A.C., Eaton, S.A. and Bolam, J.P. (1998). Selective Innervation of Neostriatal Interneurons by a Subclass of Neuron in the Globus Pallidus of the Rat. J. Neurosci. *18*, 9438–9452.

Björklund, A. and Dunnett, S.B. (2007). Dopamine neuron systems in the brain: an update. Trends in Neurosciences *30*, 194–202.

Bolam, J.P., Hanley, J.J., Booth, P. a. C. and Bevan, M.D. (2000). Synaptic organisation of the basal ganglia. Journal of Anatomy *196*, 527–542.

Calabresi, P., Centonze, D., Gubellini, P., Marfia, G.A., Pisani, A., Sancesario, G. and Bernardi, G. (2000). Synaptic transmission in the striatum: from plasticity to neurodegeneration. Progress in Neurobiology *61*, 231–265.

Callaway, E.M. (2008). Transneuronal Circuit Tracing with Neurotropic Viruses. Curr Opin Neurobiol *18*, 617–623.

Callaway, E.M. and Luo, L. (2015). Monosynaptic Circuit Tracing with Glycoprotein-Deleted Rabies Viruses. J. Neurosci. *35*, 8979–8985.

Cdc.gov,. 'CDC - Biosafety In Microbiological And Biomedical Laboratories (BMBL) 5Th Edition'. N. p., 2015. Web. 19 July 2015.

Centonze, D., Bracci, E., Pisani, A., Gubellini, P., Bernardi, G. and Calabresi, P. (2002). Activation of dopamine D1-like receptors excites LTS interneurons of the striatum. European Journal of Neuroscience *15*, 2049–2052.

Cepeda, C., Galvan, L., Holley, S.M., Rao, S.P. andré, V.M., Botelho, E.P., Chen, J.Y., Watson, J.B., Deisseroth, K. and Levine, M.S. (2013). Multiple sources of striatal inhibition are differentially affected in Huntington's disease mouse models. J. Neurosci. *33*, 7393–7406.

Chang, H.T. and Kita, H. (1992). Interneurons in the rat striatum: relationships between parvalbumin neurons and cholinergic neurons. Brain Research *574*, 307–311.

Deisseroth, K., Feng, G., Majewska, A.K., Miesenböck, G., Ting, A. and Schnitzer, M.J. (2006). Next-Generation Optical Technologies for Illuminating Genetically Targeted Brain Circuits. J Neurosci *26*, 10380.

Del'Guidice, T., Lemasson, M. and Beaulieu, J.-M. (2011). Role of beta-arrestin 2 downstream of dopamine receptors in the basal ganglia. Front. Neuroanat. *5*, 58.

DeLong, M.R. (1990). Primate models of movement disorders of basal ganglia origin. Trends in Neurosciences *13*, 281–285.

Do, J., Kim, J.-I., Bakes, J., Lee, K. and Kaang, B.-K. (2013). Functional roles of neurotransmitters and neuromodulators in the dorsal striatum. Learn. Mem. *20*, 21–28.

Drago, J., Gerfen, C.R., Lachowicz, J.E., Steiner, H., Hollon, T.R., Love, P.E., Ooi, G.T., Grinberg, A., Lee, E.J. and Huang, S.P. (1994). Altered striatal function in a mutant mouse lacking D1A dopamine receptors. Proc Natl Acad Sci U S A *91*, 12564–12568.

Ehrengruber, M.U., Lundstrom, K., Schweitzer, C., Heuss, C., Schlesinger, S. and Gähwiler, B.H. Recombinant Semliki Forest virus and Sindbis virus efficiently infect neurons in hippocampal slice cultures.

Emery, B. and Barres, B.A. (2008). Unlocking CNS Cell Type Heterogeneity. Cell *135*, 596–598.

Fenno, L., Yizhar, O. and Deisseroth, K. (2011). The Development and Application of Optogenetics. Annual Review of Neuroscience *34*, 389–412.

Gabernet, L., Jadhav, S.P., Feldman, D.E., Carandini, M. and Scanziani, M. (2005). Somatosensory Integration Controlled by Dynamic Thalamocortical Feed-Forward Inhibition. Neuron *48*, 315–327.

Galvan, A. and Wichmann, T. (2007). GABAergic circuits in the basal ganglia and movement disorders. Prog. Brain Res. *160*, 287–312.

Gertler, T.S., Chan, C.S. and Surmeier, D.J. (2008). Dichotomous Anatomical Properties of Adult Striatal Medium Spiny Neurons. J. Neurosci. *28*, 10814–10824.

Ghanem, A. and Conzelmann, K.-K. (2015). G gene-deficient single-round rabies viruses for neuronal circuit analysis. Virus Res.

Gittis, A.H. and Kreitzer, A.C. (2012). Striatal microcircuitry and movement disorders. Trends Neurosci. *35*, 557–564.

Gittis, A.H., Nelson, A.B., Thwin, M.T., Palop, J.J. and Kreitzer, A.C. (2010). Distinct Roles of GABAergic Interneurons in the Regulation of Striatal Output Pathways. J. Neurosci. *30*, 2223–2234.

Gittis, A.H., Leventhal, D.K., Fensterheim, B.A., Pettibone, J.R., Berke, J.D. and Kreitzer, A.C. (2011). Selective Inhibition of Striatal Fast-Spiking Interneurons Causes Dyskinesias. J. Neurosci. *31*, 15727–15731.

Gong, S., Zheng, C., Doughty, M.L., Losos, K., Didkovsky, N., Schambra, U.B., Nowak, N.J., Joyner, A., Leblanc, G., Hatten, M.E., et al. (2003). A gene expression atlas of the central nervous system based on bacterial artificial chromosomes. Nature *425*, 917–925.

Gong, S., Doughty, M., Harbaugh, C.R., Cummins, A., Hatten, M.E., Heintz, N. and Gerfen, C.R. (2007). Targeting Cre Recombinase to Specific Neuron Populations with Bacterial Artificial Chromosome Constructs. J. Neurosci. *27*, 9817–9823.

Graybiel, A.M. (2000). The basal ganglia. Current Biology *10*, R509–R511.

Graybiel, A.M., Aosaki, T., Flaherty, A.W. and Kimura, M. (1994). The basal ganglia and adaptive motor control. Science *265*, 1826–1831.

Guo, Q., Wang, D., He, X., Feng, Q., Lin, R., Xu, F., Fu, L. and Luo, M. (2015). Whole-brain mapping of inputs to projection neurons and cholinergic interneurons in the dorsal striatum. PLoS ONE *10*, e0123381.

Guru, A., Post, R.J., Ho, Y.-Y. and Warden, M.R. (2015). Making Sense of Optogenetics. International Journal of Neuropsychopharmacology pyv079.

Hayut, I., Fanselow, E.E., Connors, B.W. and Golomb, D. (2011). LTS and FS Inhibitory Interneurons, Short-Term Synaptic Plasticity and Cortical Circuit Dynamics. PLoS Comput Biol *7*, e1002248.

Heiman, M., Schaefer, A., Gong, S., Peterson, J., Day, M., Ramsey, K.E., Suárez-Fariñas, M., Schwarz, C., Stephan, D.A., Surmeier, D.J., et al. (2008). Development of a BACarray translational profiling approach for the molecular characterization of CNS cell types. Cell *135*, 738–748.

Hippenmeyer, S., Vrieseling, E., Sigrist, M., Portmann, T., Laengle, C., Ladle, D.R. and Arber, S. (2005). A Developmental Switch in the Response of DRG Neurons to ETS Transcription Factor Signaling. PLoS Biol *3*.

Hu, H., Gan, J. and Jonas, P. (2014). Fast-spiking, parvalbumin+ GABAergic interneurons: From cellular design to microcircuit function. Science *345*, 1255263.

Isaacson, J.S. and Scanziani, M. (2011). How Inhibition Shapes Cortical Activity. Neuron *72*, 231–243.

Kaneko, S., Hikida, T., Watanabe, D., Ichinose, H., Nagatsu, T., Kreitman, R.J., Pastan, I. and Nakanishi, S. (2000). Synaptic integration mediated by striatal cholinergic interneurons in basal ganglia function. Science *289*, 633–637.

Kawaguchi, Y. (1993). Physiological, morphological and histochemical characterization of three classes of interneurons in rat neostriatum. J. Neurosci. *13*, 4908–4923.

Kawaguchi, Y. (1997). Neostriatal cell subtypes and their functional roles. Neuroscience Research *27*, 1–8.

Kawaguchi, Y. and Kubota, Y. (1997). GABAergic cell subtypes and their synaptic connections in rat frontal cortex. Cereb. Cortex *7*, 476–486.

Kawaguchi, Y., Wilson, C.J., Augood, S.J. and Emson, P.C. (1995). Striatal interneurones: chemical, physiological and morphological characterization. Trends in Neurosciences *18*, 527–535.

Koós, T. and Tepper, J.M. (1999). Inhibitory control of neostriatal projection neurons by GABAergic interneurons. Nat. Neurosci. *2*, 467–472.

Koos, T., Tepper, J.M. and Wilson, C.J. (2004). Comparison of IPSCs Evoked by Spiny and Fast-Spiking Neurons in the Neostriatum. J. Neurosci. *24*, 7916–7922.

Korecka, J., Schouten, M., Eggers, R., Ulusoy, A., Bossers, K. and Verhaage, J. (2011). Comparison of AAV Serotypes for Gene Delivery to Dopaminergic Neurons in the Substantia Nigra. In Viral Gene Therapy, K. Xu, ed. (InTech),.

Kozorovitskiy, Y., Saunders, A., Johnson, C.A., Lowell, B.B. and Sabatini, B.L. (2012). Recurrent network activity drives striatal synaptogenesis. Nature *485*, 646–650.

Kravitz, A.V., Freeze, B.S., Parker, P.R.L., Kay, K., Thwin, M.T., Deisseroth, K. and Kreitzer, A.C. (2010). Regulation of parkinsonian motor behaviours by optogenetic control of basal ganglia circuitry. Nature *466*, 622–626.

Kreitzer, A.C. (2009). Physiology and Pharmacology of Striatal Neurons. Annual Review of Neuroscience *32*, 127–147.

Kreitzer, A.C. and Malenka, R.C. (2008). Striatal Plasticity and Basal Ganglia Circuit Function. Neuron *60*, 543–554.

Liem, L.K., Simard, J.M., Song, Y. and Tewari, K. (1995). The patch clamp technique. Neurosurgery *36*, 382–392.

Lima, S.Q., Hromádka, T., Znamenskiy, P. and Zador, A.M. (2009). PINP: A New Method of Tagging Neuronal Populations for Identification during In Vivo Electrophysiological Recording. PLoS One *4*.

Lobo, M.K. (2009). Chapter 1 - Molecular Profiling of Striatonigral and Striatopallidal Medium Spiny Neurons: Past, Present and Future. In International Review of Neurobiology, Xiao-Hong Lu, ed. (Academic Press), pp. 1–35.

Lüscher, C. and Malenka, R.C. (2011). Drug-Evoked Synaptic Plasticity in Addiction: From Molecular Changes to Circuit Remodeling. Neuron *69*, 650–663.

Madisen, L., Zwingman, T.A., Sunkin, S.M., Oh, S.W., Zariwala, H.A., Gu, H., Ng, L.L., Palmiter, R.D., Hawrylycz, M.J., Jones, A.R., et al. (2010). A robust and high-throughput Cre reporting and characterization system for the whole mouse brain. Nat Neurosci *13*, 133–140.

Mallet, N., Ballion, B., Moine, C.L. and Gonon, F. (2006). Cortical Inputs and GABA Interneurons Imbalance Projection Neurons in the Striatum of Parkinsonian Rats. J. Neurosci. *26*, 3875–3884.

Marín, O. anderson, S.A. and Rubenstein, J.L.R. (2000). Origin and Molecular Specification of Striatal Interneurons. J. Neurosci. *20*, 6063–6076.

Matamales, M., Bertran-Gonzalez, J., Salomon, L., Degos, B., Deniau, J.-M., Valjent, E., Herve, D. and Girault, J.-A. (2009). Striatal Medium-Sized Spiny Neurons: Identification by Nuclear Staining and Study of Neuronal Subpopulations in BAC Transgenic Mice. PLoS ONE *4*.

McBain, C.J. and Fisahn, A. (2001). Interneurons unbound. Nat. Rev. Neurosci. *2*, 11–23.

McHaffie, J.G., Stanford, T.R., Stein, B.E., Coizet, V. and Redgrave, P. (2005). Subcortical loops through the basal ganglia. Trends in Neurosciences *28*, 401–407.

Meck, W.H., Penney, T.B. and Pouthas, V. (2008). Cortico-striatal representation of time in animals and humans. Current Opinion in Neurobiology *18*, 145–152.

MINK, J.W. (1996). The Basal Ganglia: Focused selection and inhibition of competing motor programs. Progress in Neurobiology *50*, 381–425.

Nambu, A. (2008). Seven problems on the basal ganglia. Current Opinion in Neurobiology *18*, 595–604.

Nathanson, J.L., Jappelli, R., Scheeff, E.D., Manning, G., Obata, K., Brenner, S., Callaway, E.M., Nathanson, J.L., Jappelli, R., Scheeff, E.D., et al. (2009). Short promoters in viral vectors drive selective expression in mammalian inhibitory neurons, but do not restrict activity to specific inhibitory cell-types. Front. Neural Circuits *3*, 19.

Nelson, A.B. and Kreitzer, A.C. (2014). Reassessing models of basal ganglia function and dysfunction. Annu. Rev. Neurosci. *37*, 117–135.

Neuroscience.uth.tmc.edu,.(1) 'Basal Ganglia (Section 3, Chapter 4) Neuroscience Online: An Electronic Textbook For The Neurosciences | Department Of Neurobiology And Anatomy - The University Of Texas Medical School At Houston'. N. p., 2015. Web. 18 June 2015.

Neuroscience.uth.tmc.edu,.(2) 'Introduction To Neurons And Neuronal Networks | Section 1, Intro Chapter | Neuroscience Online: An Electronic Textbook For The Neurosciences | Department Of Neurobiology And Anatomy - The University Of Texas Medical School At Houston'. N. p., 2015. Web. 18 June 2015.

Oldenburg, I.A. and Ding, J.B. (2011). Cholinergic modulation of synaptic integration and dendritic excitability in the striatum. Curr Opin Neurobiol *21*, 425–432.

Oldenburg, I.A. and Sabatini, B.L. (2015). Antagonistic but Not Symmetric Regulation of Primary Motor Cortex by Basal Ganglia Direct and Indirect Pathways. Neuron *86*, 1174–1181.

Osakada, F. and Callaway, E.M. (2013). Design and generation of recombinant rabies virus vectors. Nat Protoc *8*, 1583–1601.

Pisani, A., Bernardi, G., Ding, J. and Surmeier, D.J. (2007). Re-emergence of striatal cholinergic interneurons in movement disorders. Trends in Neurosciences *30*, 545–553.

Planert, H., Szydlowski, S.N., Hjorth, J.J.J., Grillner, S. and Silberberg, G. (2010). Dynamics of Synaptic Transmission between Fast-Spiking Interneurons and Striatal Projection Neurons of the Direct and Indirect Pathways. J. Neurosci. *30*, 3499–3507.

Ramanathan, S., Hanley, J.J., Deniau, J.-M. and Bolam, J.P. (2002). Synaptic Convergence of Motor and Somatosensory Cortical Afferents onto GABAergic Interneurons in the Rat Striatum. J. Neurosci. *22*, 8158–8169.

Redgrave, P., Rodriguez, M., Smith, Y., Rodriguez-Oroz, M.C., Lehericy, S., Bergman, H., Agid, Y., DeLong, M.R. and Obeso, J.A. (2010). Goal-directed and habitual control in the basal ganglia: implications for Parkinson's disease. Nature Reviews Neuroscience *11*, 760–772.

Reid, M.S., Herrera-Marschitz, M., Hökfelt, T., Lindefors, N., Persson, H. and Ungerstedt, U. (1990). Striatonigral GABA, dynorphin, substance P and neurokinin A modulation of nigrostriatal dopamine release: evidence for direct regulatory mechanisms. Exp Brain Res *82*, 293–303.

Rikani, A.A., Choudhry, Z., Choudhry, A.M., Rizvi, N., Ikram, H., Mobassarah, N.J. and Tulli, S. (2014). The mechanism of degeneration of striatal neuronal subtypes in Huntington disease. Ann Neurosci *21*, 112–114.

Schmidt, E.F., Kus, L., Gong, S. and Heintz, N. (2013). BAC Transgenic Mice and the GENSAT Database of Engineered Mouse Strains. Cold Spring Harb Protoc *2013*, pdb.top073692.

Shen, H.-Y., Coelho, J.E., Ohtsuka, N., Canas, P.M., Day, Y.-J., Huang, Q.-Y., Rebola, N., Yu, L., Boison, D., Cunha, R.A., et al. (2008). A Critical Role of the Adenosine A2A Receptor in Extrastriatal Neurons in Modulating Psychomotor Activity as Revealed by Opposite Phenotypes of Striatum and Forebrain A2A Receptor Knock-Outs. J. Neurosci. *28*, 2970–2975.

Shepherd, G.M.G. (2013). Corticostriatal connectivity and its role in disease. Nat Rev Neurosci *14*, 278–291.

Shuen, J.A., Chen, M., Gloss, B. and Calakos, N. (2008). Drd1a-tdTomato BAC Transgenic Mice for Simultaneous Visualization of Medium Spiny Neurons in the Direct and Indirect Pathways of the Basal Ganglia. J. Neurosci. *28*, 2681–2685.

Smith, Y., Bevan, M.D., Shink, E. and Bolam, J.P. (1998). Microcircuitry of the direct and indirect pathways of the basal ganglia. Neuroscience *86*, 353–387.

Sreenivasan, V., Karmakar, K., Rijli, F.M. and Petersen, C.C.H. (2015). Parallel pathways from motor and somatosensory cortex for controlling whisker movements in mice. Eur. J. Neurosci. *41*, 354–367.

Stoessl, A.J., Lehericy, S. and Strafella, A.P. (2014). Imaging insights into basal ganglia function, Parkinson's disease and dystonia. The Lancet *384*, 532–544.

Straub, C., Tritsch, N.X., Hagan, N.A., Gu, C. and Sabatini, B.L. (2014). Multiphasic Modulation of Cholinergic Interneurons by Nigrostriatal Afferents. J. Neurosci. *34*, 8557–8569.

Taniguchi, H., He, M., Wu, P., Kim, S., Paik, R., Sugino, K., Kvitsani, D., Fu, Y., Lu, J., Lin, Y., et al. (2011). A Resource of Cre Driver Lines for Genetic Targeting of GABAergic Neurons in Cerebral Cortex. Neuron *71*, 995–1013.

Taverna, S., Ilijic, E. and Surmeier, D.J. (2008). Recurrent Collateral Connections of Striatal Medium Spiny Neurons Are Disrupted in Models of Parkinson's Disease. J. Neurosci. *28*, 5504–5512.

Tepper, J.M. and Bolam, J.P. (2004). Functional diversity and specificity of neostriatal interneurons. Current Opinion in Neurobiology *14*, 685–692.

Tepper, J. and Plenz, D. (2006). Microcircuits in the striatum: Striatal cell types and their interaction. In Microcircuits: The Interface between Neurons and Global Brain Function (Dahlem Workshop Reports), S. Grillner and A. Graybiel, eds. (The MIT Press),.

Tepper, J.M., Koós, T. and Wilson, C.J. (2004). GABAergic microcircuits in the neostriatum. Trends in Neurosciences *27*, 662–669.

Tepper, J.M., Tecuapetla, F., Koós, T. and Ibáñez-Sandoval, O. (2010). Heterogeneity and Diversity of Striatal GABAergic Interneurons. Front Neuroanat *4*.

Theriault, E. and Landis, D.M.D. (1987). Morphology of striatal neurons containing VIP-like immunoreactivity. J. Comp. Neurol. *256*, 1–13.

Tritsch, N.X. and Sabatini, B.L. (2012). Dopaminergic Modulation of Synaptic Transmission in Cortex and Striatum. Neuron *76*, 33–50.

Ugolini, G. (2011). Rabies virus as a transneuronal tracer of neuronal connections. Adv. Virus Res. *79*, 165–202.

Vincent, S.R., Staines, W.A. and Fibiger, H.C. (1983). Histochemical demonstration of separate populations of somatostatin and cholinergic neurons in the rat striatum. Neuroscience Letters *35*, 111–114.

Wall, N.R., De La Parra, M., Callaway, E.M. and Kreitzer, A.C. (2013a). Differential Innervation of Direct- and Indirect-Pathway Striatal Projection Neurons. Neuron *79*, 347–360.

Wall, N.R., De La Parra, M., Callaway, E.M. and Kreitzer, A.C. (2013b). Differential Innervation of Direct- and Indirect-Pathway Striatal Projection Neurons. Neuron *79*, 347–360.

Wickens, J.R. (2009). Synaptic plasticity in the basal ganglia. Behavioural Brain Research *199*, 119–128.

Wickersham, I.R., Lyon, D.C., Barnard, R.J.O., Mori, T., Finke, S., Conzelmann, K.-K., Young, J.A.T. and Callaway, E.M. (2007). Monosynaptic Restriction of Transsynaptic Tracing from Single, Genetically Targeted Neurons. Neuron *53*, 639–647.

Wilson, C.J. (2007). GABAergic inhibition in the neostriatum. In Progress in Brain Research, E.D.A. and J.P.B. James M. Tepper, ed. (Elsevier), pp. 91–110.

Xu, X., Roby, K.D. and Callaway, E.M. (2010). Immunochemical characterization of inhibitory mouse cortical neurons: Three chemically distinct classes of inhibitory cells. J Comp Neurol *518*, 389–404.

Yang, X.W. and Gong, S. (2001). An Overview on the Generation of BAC Transgenic Mice for Neuroscience Research. In Current Protocols in Neuroscience, (John Wiley & Sons, Inc.),.

Yelnik, J. (2008). Modeling the organization of the basal ganglia. Revue Neurologique *164*, 969–976.

Yin, H.H. and Knowlton, B.J. (2006). The role of the basal ganglia in habit formation. Nat Rev Neurosci *7*, 464–476.

Yizhar, O., Fenno, L., Zhang, F., Hegemann, P. and Diesseroth, K. (2011). Microbial Opsins: A Family of Single-Component Tools for Optical Control of Neural Activity. Cold Spring Harb Protoc *2011*, top102.

Yu, C., Gupta, J., Chen, J.-F. and Yin, H.H. (2009). Genetic deletion of A2A adenosine receptors in the striatum selectively impairs habit formation. J Neurosci *29*, 15100–15103.

Zampieri, N., Jessell, T.M. and Murray, A.J. (2014). Mapping sensory circuits by anterograde trans-synaptic transfer of recombinant rabies virus. Neuron *81*, 766–778.

Zhao, Z., Sagare, A.P., Ma, Q., Halliday, M.R., Kong, P., Kisler, K., Winkler, E.A., Ramanathan, A., Kanekiyo, T., Bu, G., et al. (2015). Central role for PICALM in amyloid-β blood-brain barrier transcytosis and clearance. Nature Neuroscience *18*, 978–987.